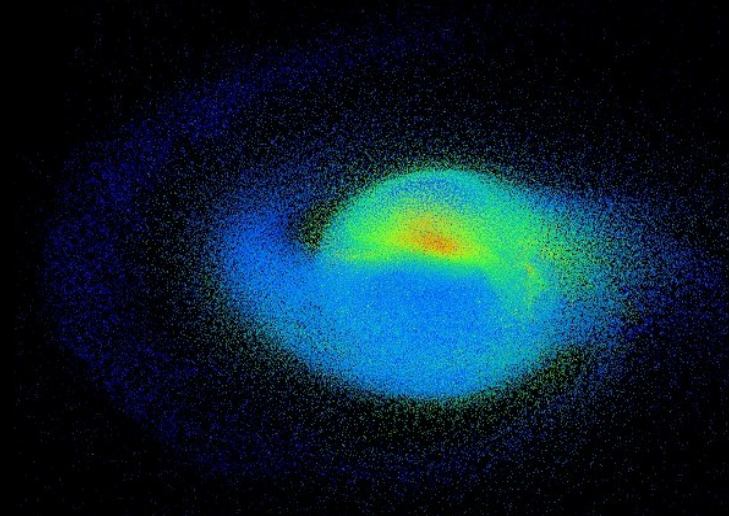
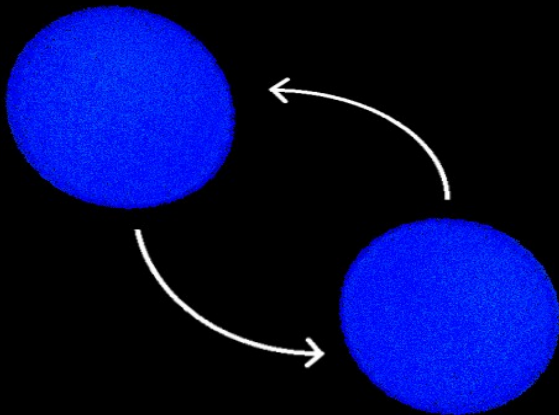


# Postmerger physics: nature of the central object – kilonova ejecta

Les Houches, 15/05/2018

Andreas Bauswein (Heidelberg Institute for Theoretical Studies)

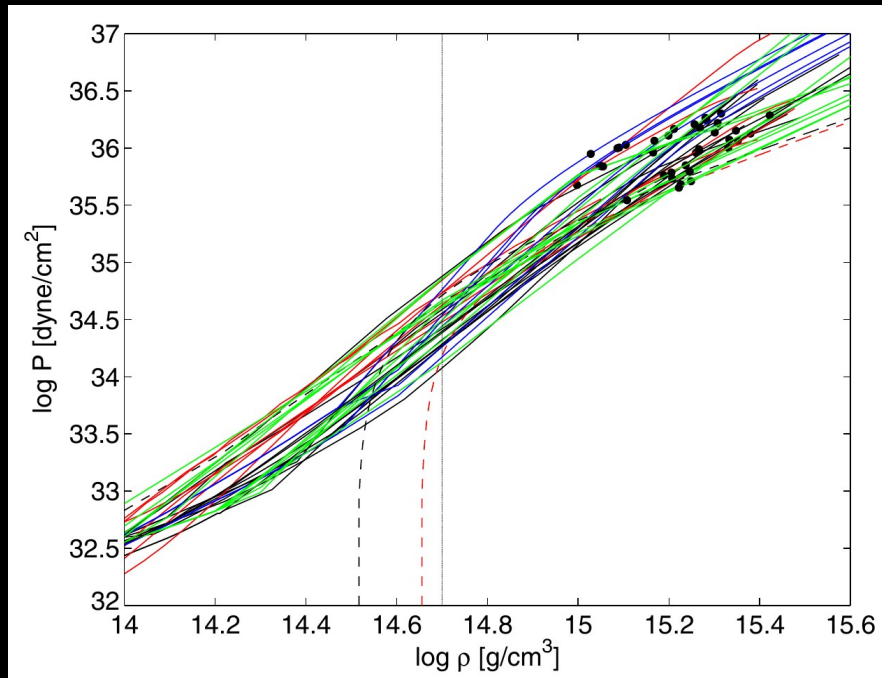


# Plan

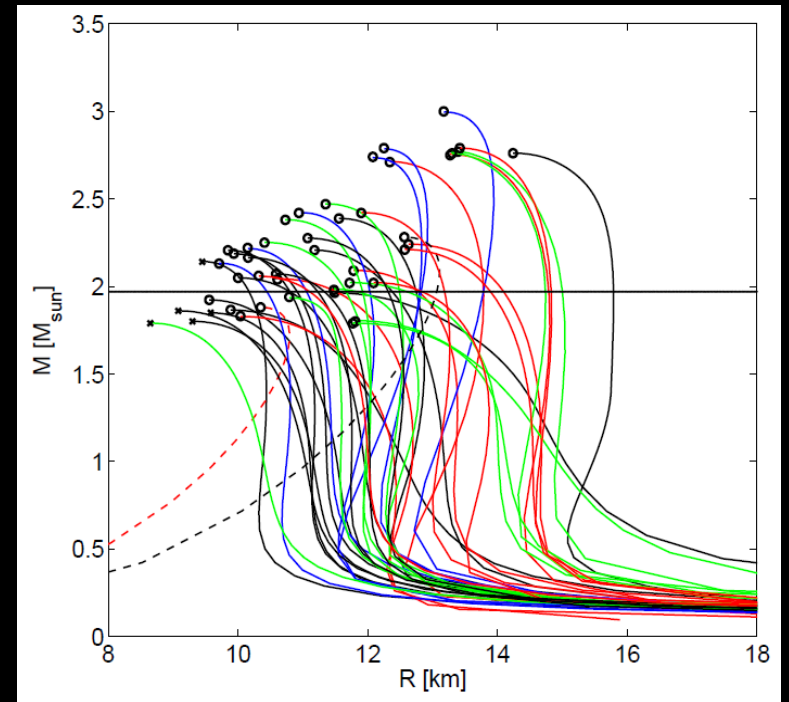
- ▶ Goal: compare observations with theory/simulations → infer unknown physics
  - e.g. role of mergers for Galactic enrichment, high-density EoS, NS properties
- ▶ Outline:
  - observations
  - ejecta from NS merger simulation
  - rates
  - collapse behavior of NS merger remnants
  - NS radius constraints from collapse behavior

# Introductory remark

- ▶ Mass-radius relation (of non-rotating NSs) and EoS are uniquely linked through Tolman-Oppenheimer-Volkoff (TOV) equations



TOV



Theory:  $P(\rho)$   $\longleftrightarrow$  currently  
future  $\longleftrightarrow$  Observation:  $R(M)$

- NS properties (of non-rotating stars) and EoS properties are equivalent !!!  
(not all displayed EoS compatible with all current constraints)

# Some insights from GW170817

- ▶ Binary masses measured from “inspiral” (= pre-merger phase with shrinking orbit)
- ▶ Detection at 40 Mpc → rate is presumably high !
- ▶ Note: chirp mass accurately measured
- ▶ Mass ratio only at higher PN order

$$\mathcal{M}_{chirp} = \frac{(M_1 M_2)^{3/5}}{(M_1 + M_2)^{1/5}}$$

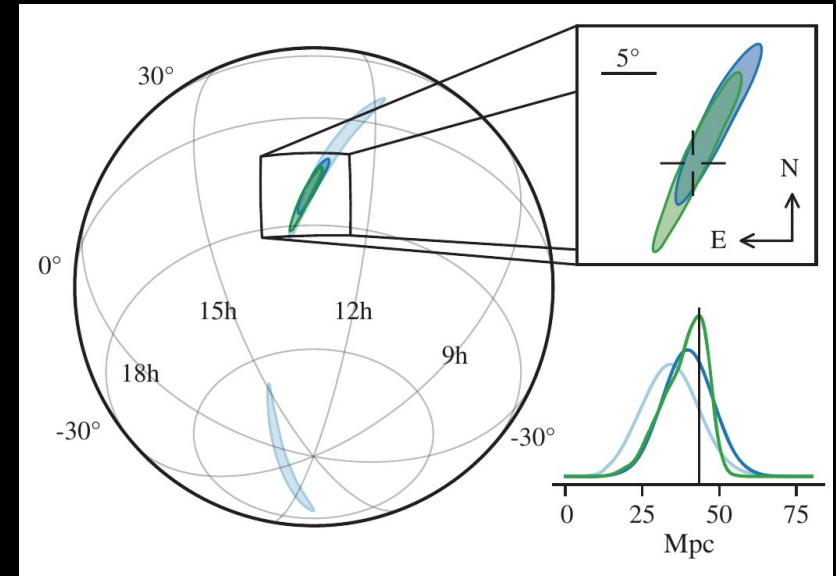
$$q = M_1/M_2$$

Abbott et al. 2017

	Low-spin priors ( $ \chi  \leq 0.05$ )	High-spin priors ( $ \chi  \leq 0.89$ )
Primary mass $m_1$	1.36–1.60 $M_\odot$	1.36–2.26 $M_\odot$
Secondary mass $m_2$	1.17–1.36 $M_\odot$	0.86–1.36 $M_\odot$
Chirp mass $\mathcal{M}$	1.188 $^{+0.004}_{-0.002}$ $M_\odot$	1.188 $^{+0.004}_{-0.002}$ $M_\odot$
Mass ratio $m_2/m_1$	0.7–1.0	0.4–1.0
Total mass $m_{tot}$	2.74 $^{+0.04}_{-0.01}$ $M_\odot$	2.82 $^{+0.47}_{-0.09}$ $M_\odot$
Radiated energy $E_{rad}$	$> 0.025 M_\odot c^2$	$> 0.025 M_\odot c^2$
Luminosity distance $D_L$	40 $^{+8}_{-14}$ Mpc	40 $^{+8}_{-14}$ Mpc
Viewing angle $\Theta$	$\leq 55^\circ$	$\leq 56^\circ$
Using NGC 4993 location	$\leq 28^\circ$	$\leq 28^\circ$
Combined dimensionless tidal deformability $\tilde{\Lambda}$	$\leq 800$	$\leq 700$
Dimensionless tidal deformability $\Lambda(1.4M_\odot)$	$\leq 800$	$\leq 1400$

# Observations

- ▶ Localization through Gw signal
  - ▶ Follow up observation (UV, optical, IR) starting ~12 h after merger
- ejecta masses, velocities, opacities



Abbott et al. 2017

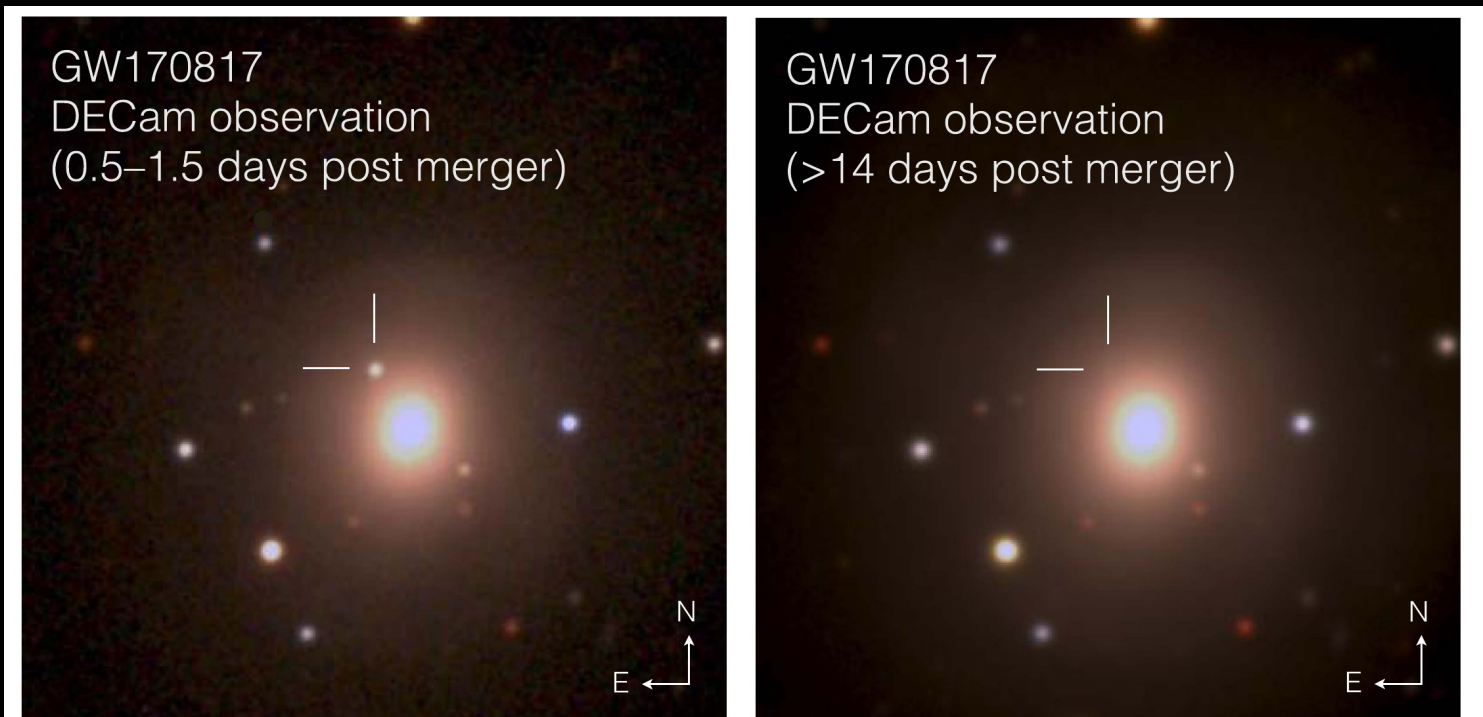
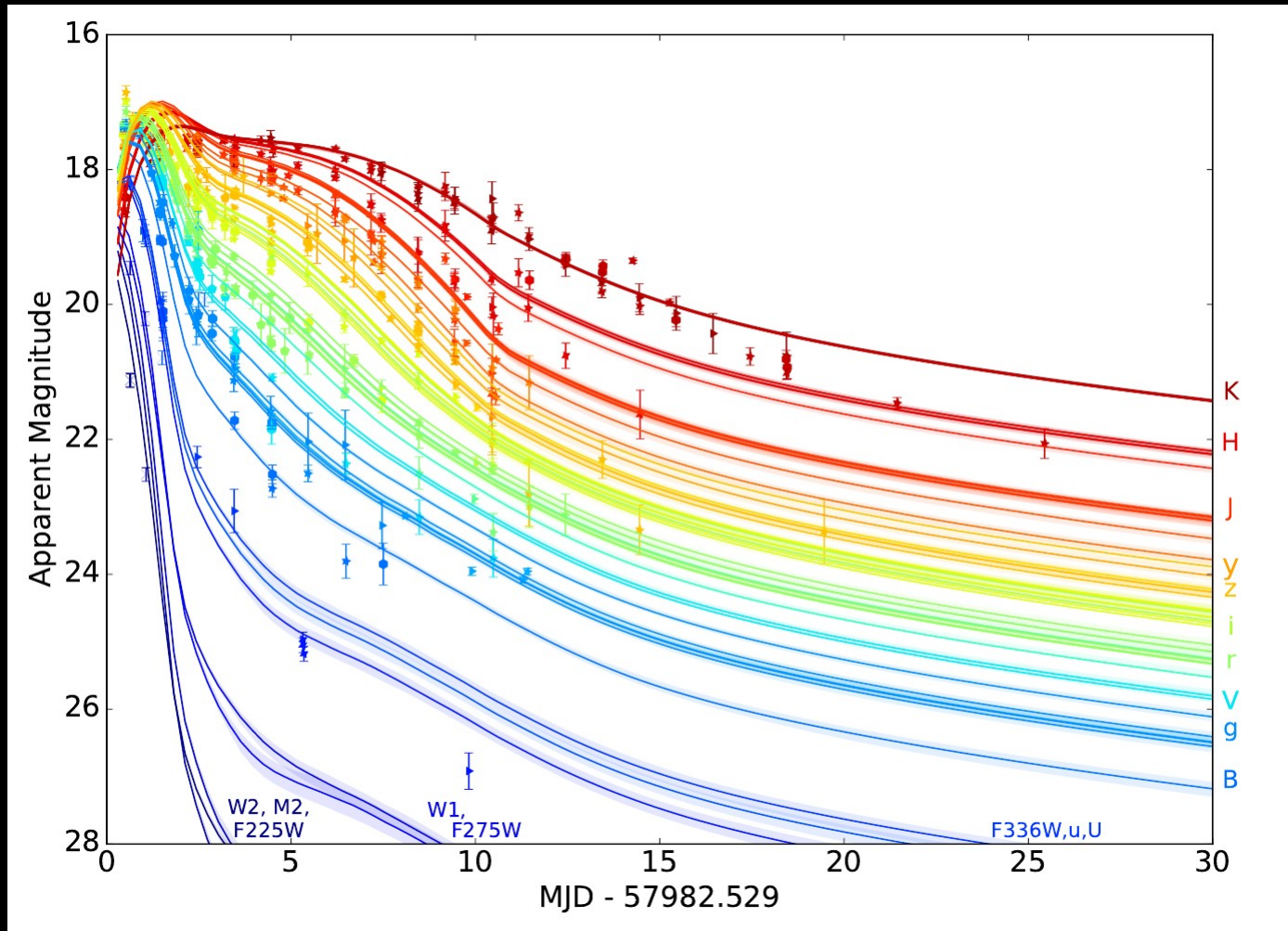


**Figure 1.** NGC4993 *grz* color composites ( $1.5 \times 1.5$ ). Left: composite of detection images, including the discovery *z* image taken on 2017 August 18 00:05:23 UT and the *g* and *r* images taken 1 day later; the optical counterpart of GW170817 is at R.A., decl. =197.450374, -23.381495. Right: the same area two weeks later.

Soares-Santos et al 2017



# Observations UVOIR – combined from different groups/observations



- ▶ From early blue to red
- ▶ Solid lines: spherical 3-components model: blue, purple, red
- ▶ Reasonable agreement

Villar et al. 2018

# Light curve interpretation

- ▶ Different modeling → overall good agreement with theoretical expectations (later)
- ▶ blue + (purple) + red component, i.e. low-opacity material + high opacity material
  - component without / with lanthanides (heavy r-process elements)
  - component with high  $Y_e$  ( $> \sim 0.25$ ) / low  $Y_e$

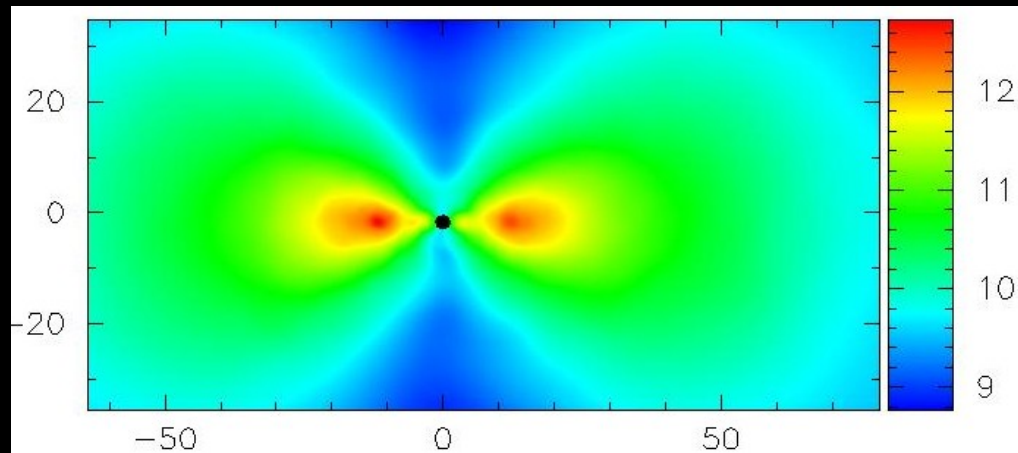
Villar et al. 2018

Model	$M_{ej}^{blue}$	$v_{ej}^{blue}$	$\kappa_{ej}^{blue}$	$T^{blue}$	$M_{ej}^{purple}$	$v_{ej}^{purple}$	$\kappa_{ej}^{purple}$	$T^{purple}$	$M_{ej}^{red}$	$v_{ej}^{red}$	$\kappa_{ej}^{red}$	$T^{red}$	$\sigma$	$\theta$	WAIC
2-Comp	$0.023_{0.001}^{0.005}$	$0.256_{0.002}^{0.005}$	(0.5)	$3983_{70}^{66}$	-	-	-	-	$0.050_{0.001}^{0.001}$	$0.149_{0.002}^{0.001}$	$3.65_{0.28}^{0.09}$	$1151_{72}^{45}$	$0.256_{0.004}^{0.006}$	-	-1030
3-Comp	$0.020_{0.001}^{0.001}$	$0.266_{0.008}^{0.008}$	(0.5)	$674_{417}^{486}$	$0.047_{0.002}^{0.001}$	$0.152_{0.005}^{0.005}$	(3)	$1308_{34}^{42}$	$0.011_{0.001}^{0.002}$	$0.137_{0.021}^{0.025}$	(10)	$3745_{75}^{75}$	$0.242_{0.008}^{0.008}$	-	-1064
Asym. 3-Comp	$0.009_{0.001}^{0.001}$	$0.256_{0.004}^{0.009}$	(0.5)	$3259_{306}^{302}$	$0.007_{0.001}^{0.001}$	$0.103_{0.004}^{0.007}$	(3)	$3728_{178}^{94}$	$0.026_{0.002}^{0.004}$	$0.175_{0.008}^{0.011}$	(10)	$1091_{45}^{29}$	$0.226_{0.006}^{0.006}$	$66_3^1$	-1116

See also Chronock et al. 2017, Levan & Tanvir 2017, Kasliwal et al. 2017, Coulter et al. 2017, Allam et al. 2017, Yang et al. 2017, Arcavi et al. 2017, Kilpatrick et al. 2017, McCully et al. 2017, Pian et al. 2017, Arcavi et al. 2017, Evans et al. 2017, Drout et al. 2017 Lipunov et al. 2017, Cowperthwaite et al. 2017, Smarr et al. 2017, Shappee et al. 2017, Nicholl et al. 2017, Kasen et al. 2017, Tanaka et al. 2017, .....

# Light curve interpretation

- ▶ Interpretation of observational data slightly differs between different groups
- ▶ But overall good agreement with theoretical expectations
- ▶ Strong evidence for ejecta heated by rapid neutron-capture process (see Stephane's talk)
- ▶ In total 0.03 ... 0.05 Msun of ejecta (= dynamical + secular ejecta)
- ▶ High ejecta mass compared to simulations

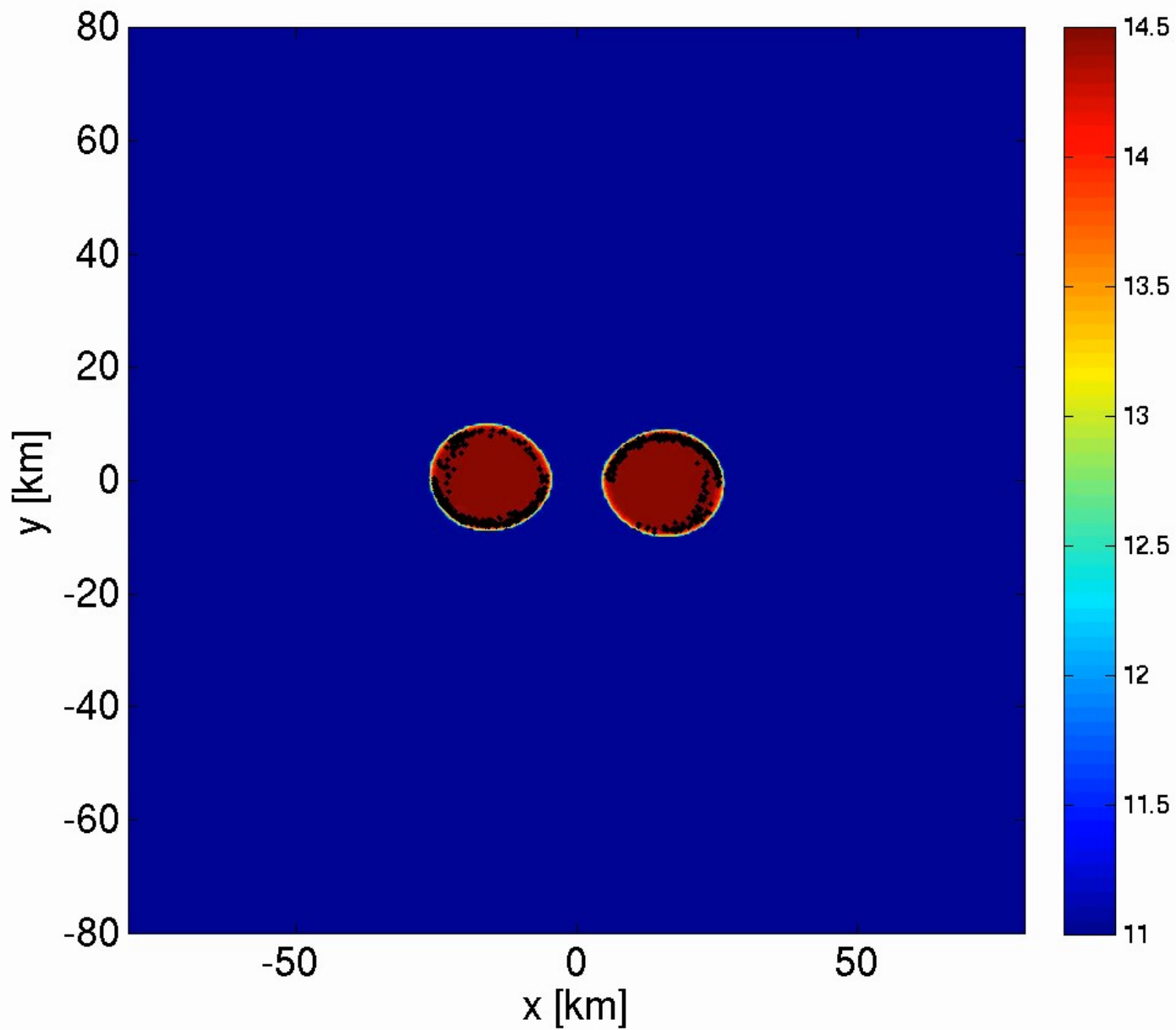


Reference	$m_{\text{dyn}} [M_{\odot}]$	$m_{\text{w}} [M_{\odot}]$
Abbott et al. (2017a)	0.001 – 0.01	–
Arcavi et al. (2017)	–	0.02 – 0.025
Cowperthwaite et al. (2017)	0.04	0.01
Chornock et al. (2017)	0.035	0.02
Evans et al. (2017)	0.002 – 0.03	0.03 – 0.1
Kasen et al. (2017)	0.04	0.025
Kasliwal et al. (2017b)	> 0.02	> 0.03
Nicholl et al. (2017)	0.03	–
Perego et al. (2017)	0.005 – 0.01	$10^{-5}$ – 0.024
Rosswog et al. (2017)	0.01	0.03
Smartt et al. (2017)	0.03 – 0.05	0.018
Tanaka et al. (2017a)	0.01	0.03
Tanvir et al. (2017)	0.002 – 0.01	0.015
Troja et al. (2017)	0.001 – 0.01	0.015 – 0.03



# Simulation results – ejecta

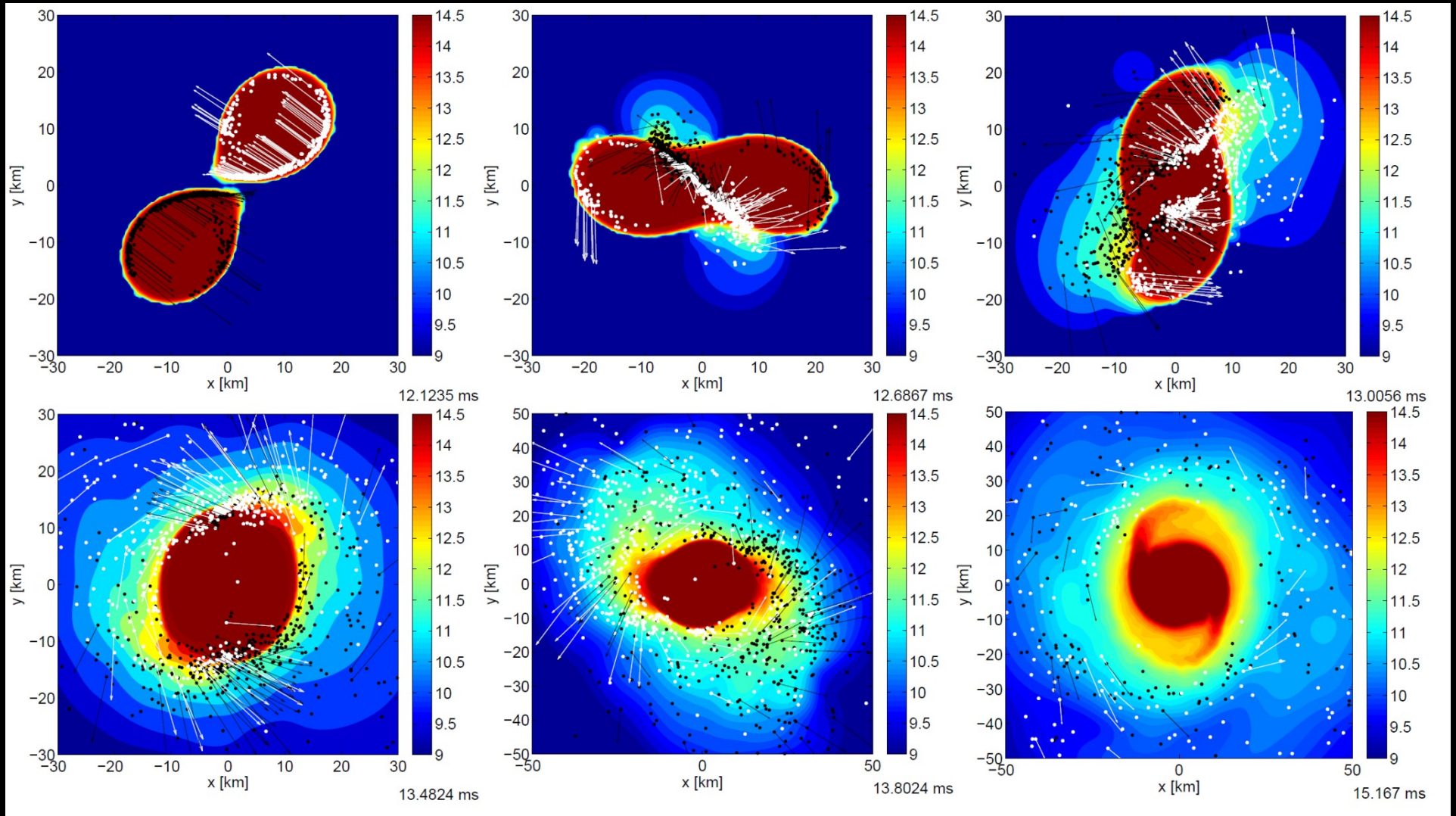
(EoS and binary mass dependence)



DD2 1.35-1.35  $M_{\text{sun}}$ , representative ejecta particles (white unbound)

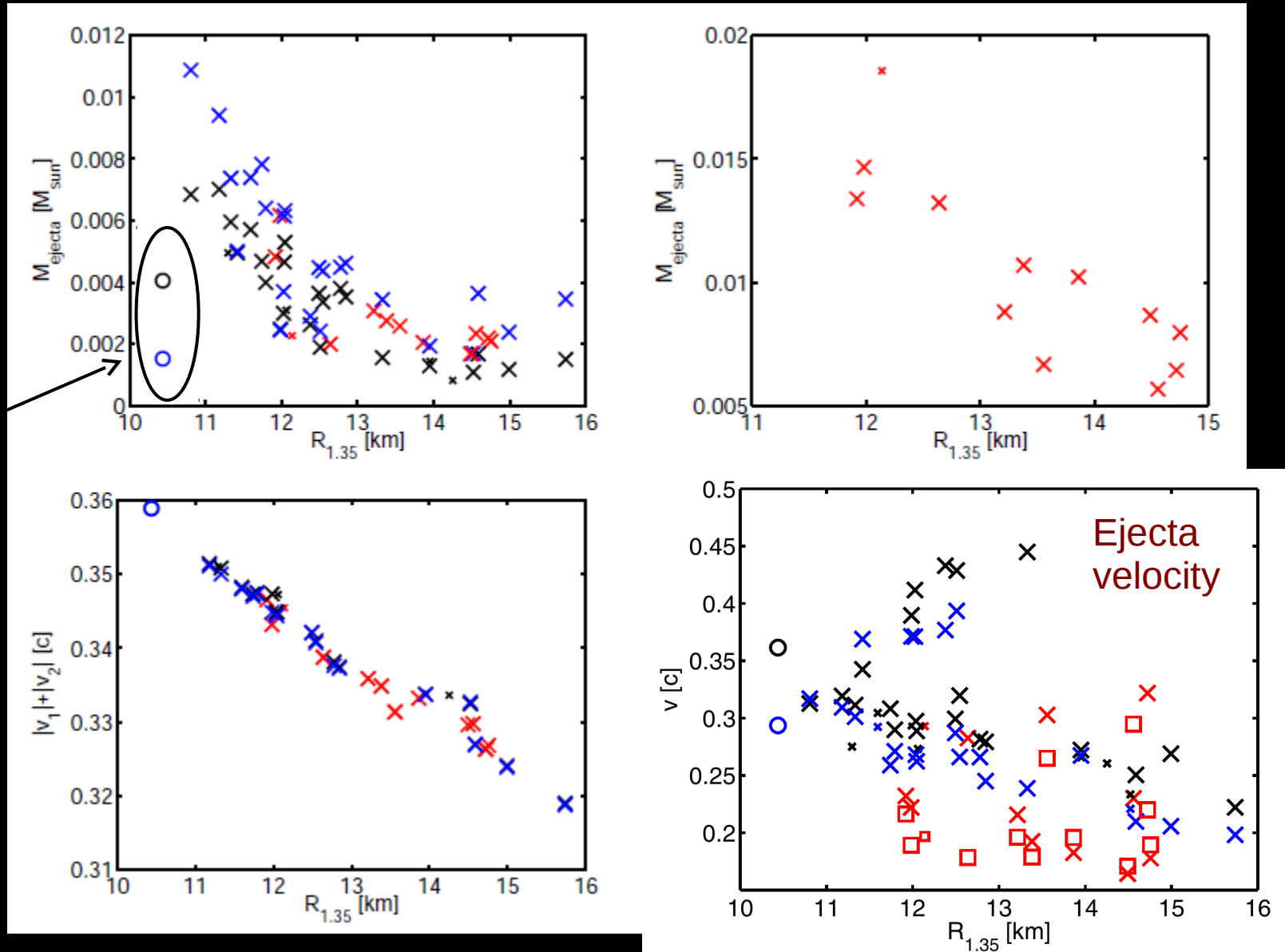
# Simulations

Dots trace ejecta (DD2 EoS 1.35-1.35  $M_{\text{sun}}$ )



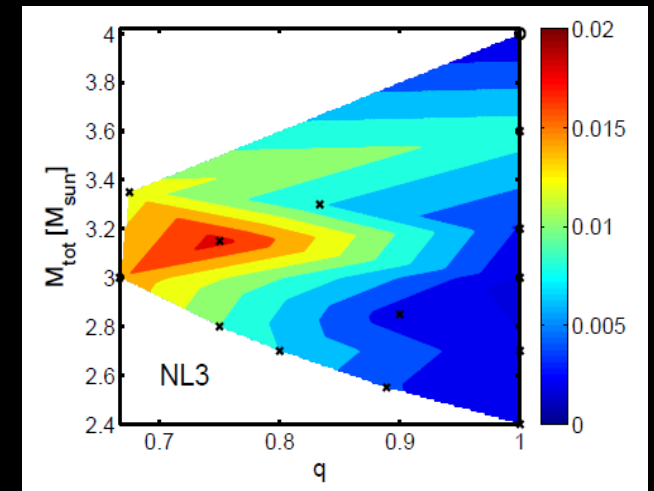
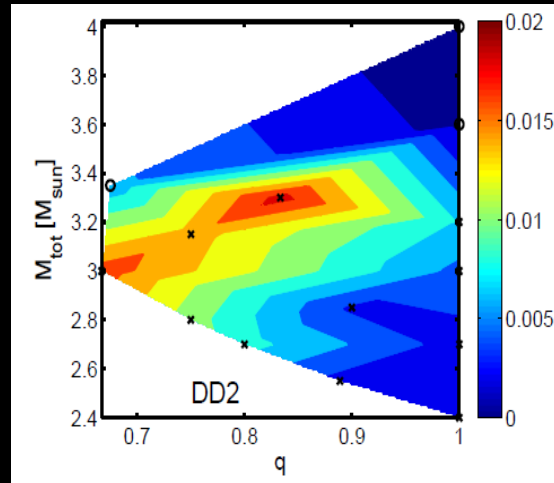
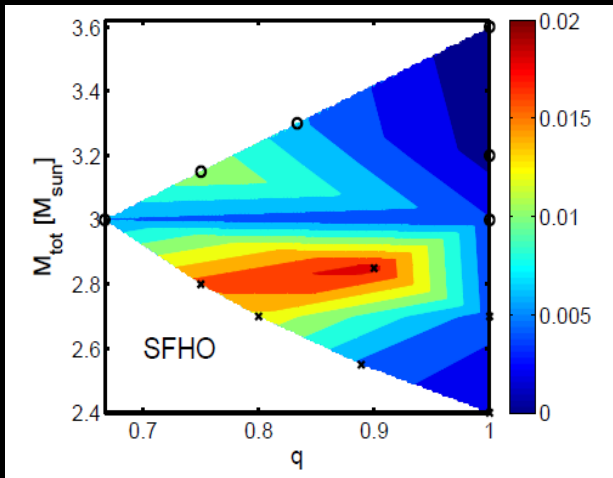
# Ejecta mass dependence

Prompt collapse



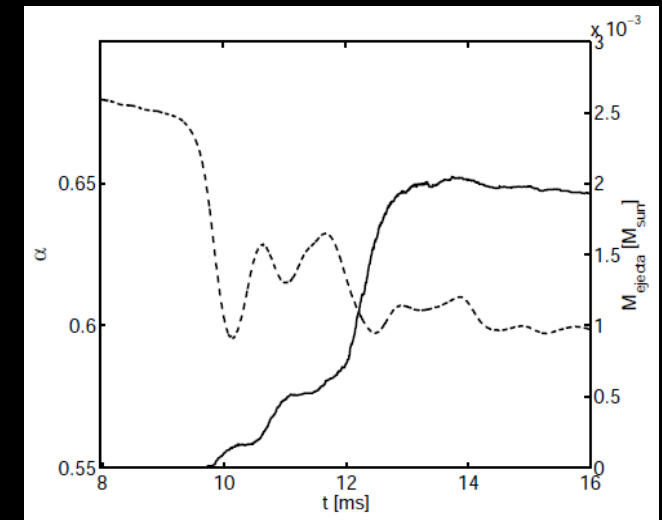
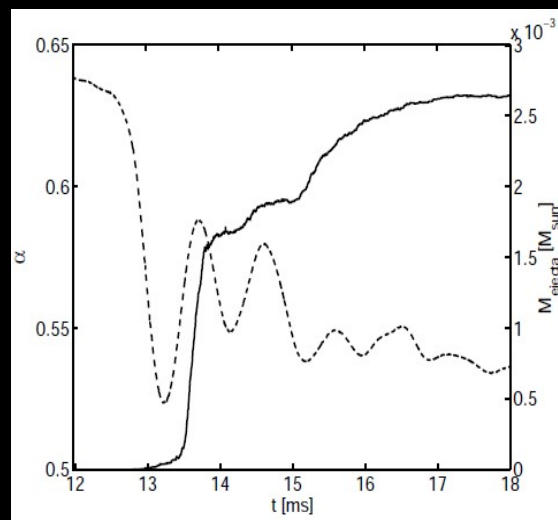
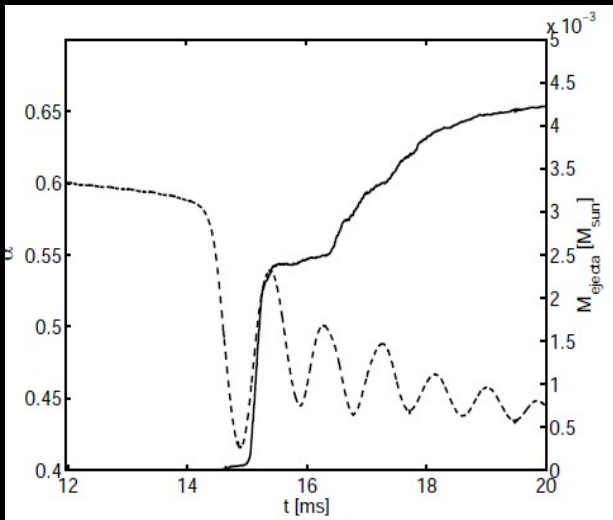
Different EoSs characterized by radii of  $1.35 M_{\text{sun}}$  NSs (note importance of thermal effects)

# Ejecta mass dependencies: binary para.



Stiffness

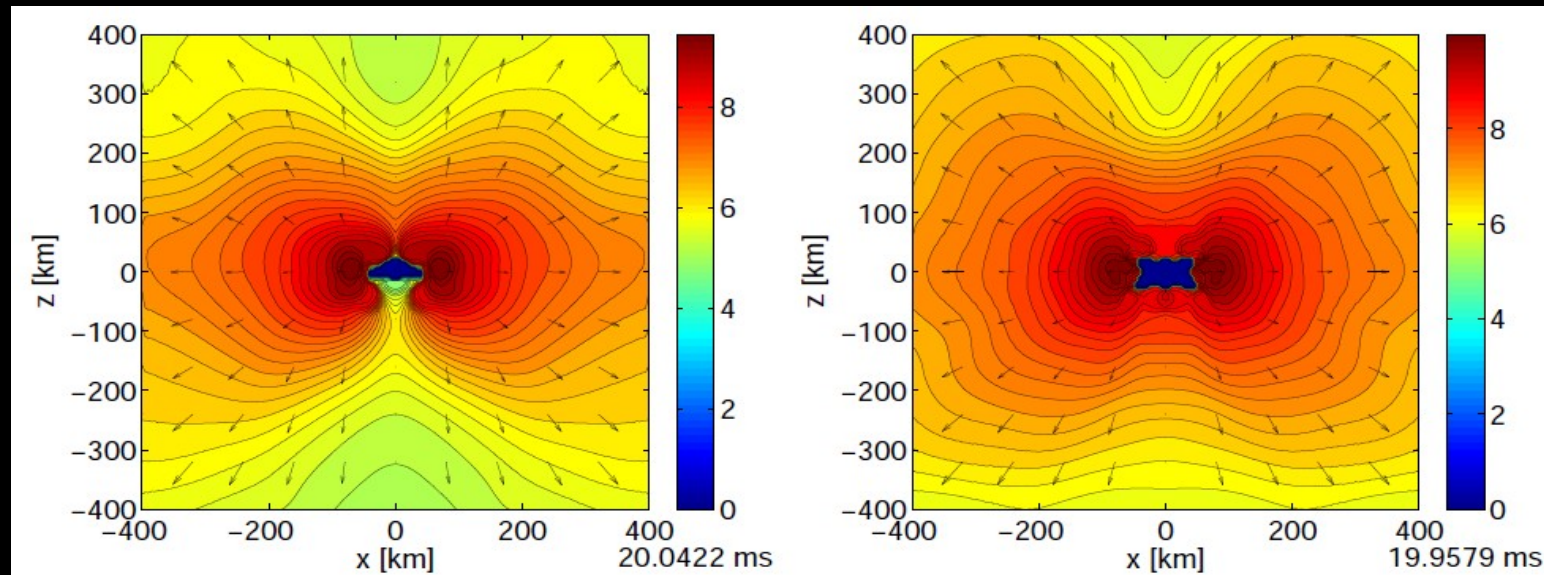
understandable by different dynamics / impact velocity / postmerger oscillations



Central lapse  $\alpha$  traces remnant compactness / oscillations / dynamics (dashed lines)

# Ejecta morphology

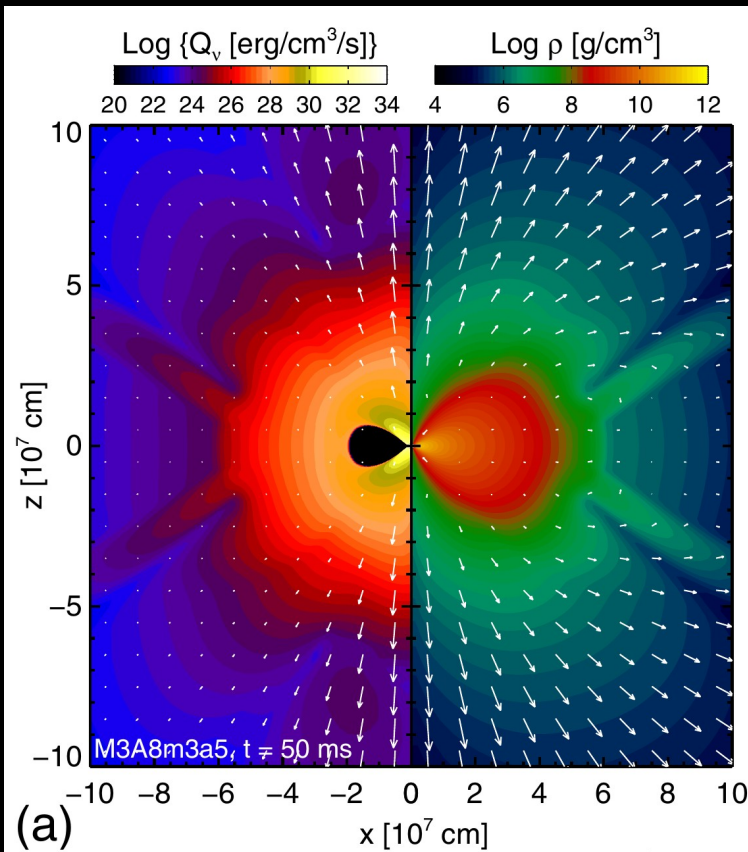
- Robust features: **fast expansion (a few 10 % c)**, **neutron rich** (neutrinos effects may lead to a broader distribution of  $Y_e$ , see Wanajo et al. 2014) (ejecta originates from inner neutron crust (initial  $Y_e$  very low))
- Rather isotropic ejection → dynamical ejecta obscures secular ejecta → early blue component puzzling? → strong neutrino effects such that no heavy r-process elements (high opacity material is produced)?
- r-process nucleosynthesis → Stephane's talk



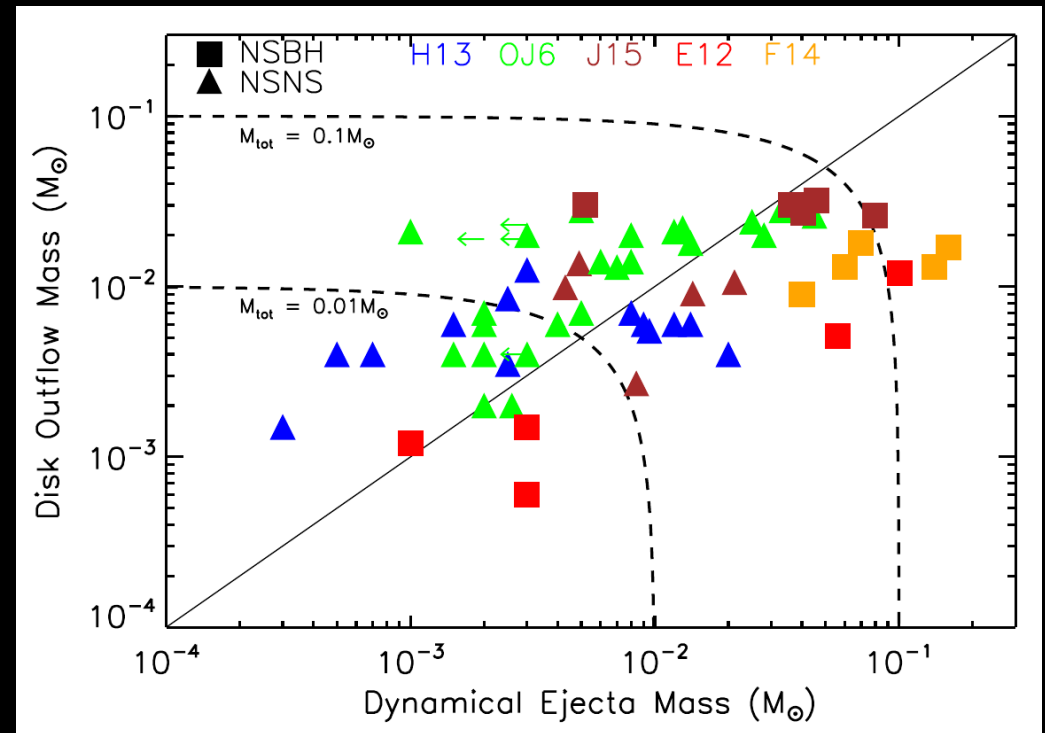


# Secular ejecta

- ▶ Remnant: BH-torus or NS + torus → secular ejecta (neutrino driven, viscously driven)
  - a few to several 10 % of the torus mass unbound
  - tentatively somewhat slower ( $\sim 0.1 c$ ) and less neutron rich → production of lighter r-process elements



Torus simulation – Just et al. 2015



Compilation by Wu et al. 2016

Rates – Are mergers dominant source of heavy r-process elements?

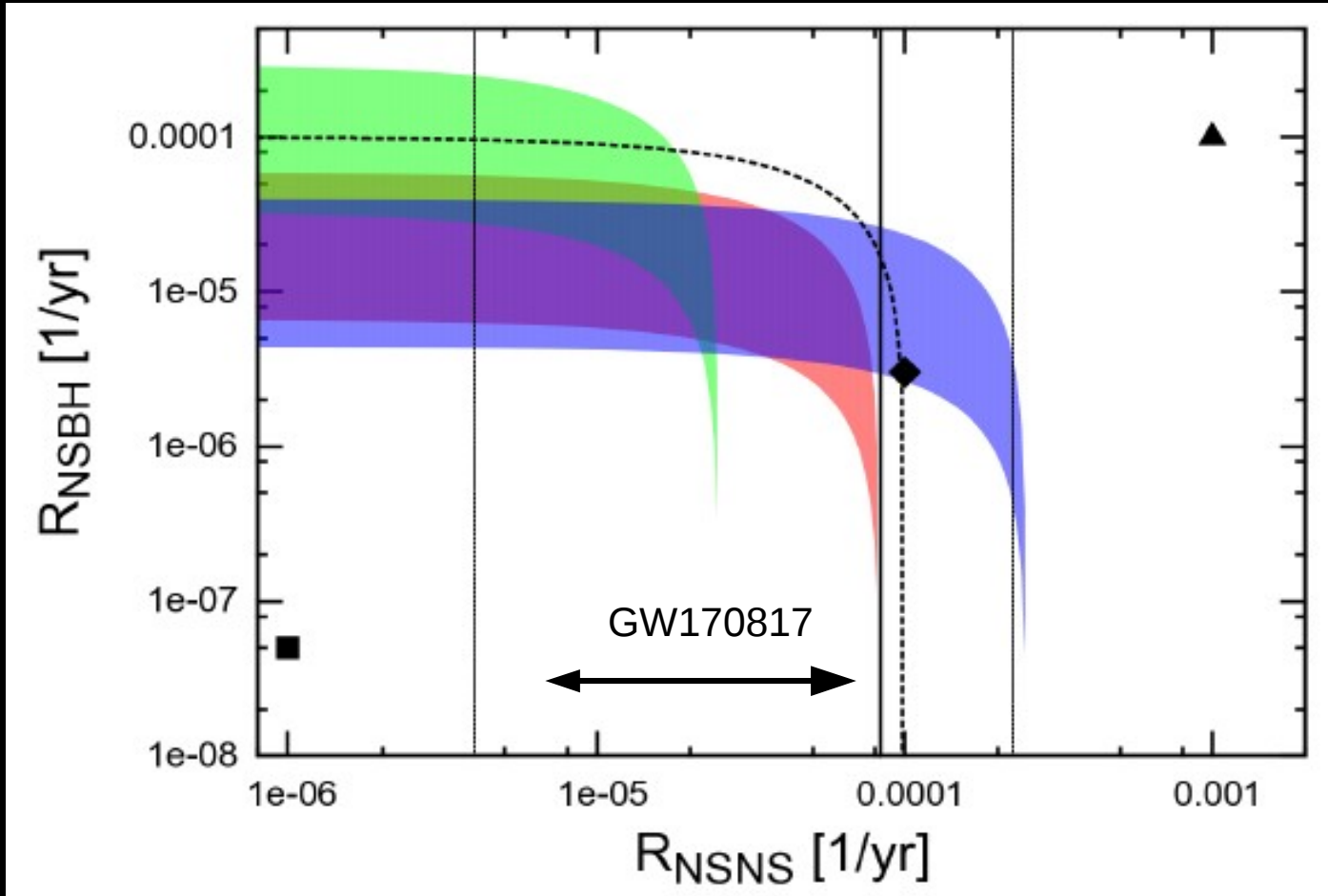
# Rates

- ▶ Could NS mergers be the (dominant) source of heavy r-process elements? \*
- ▶ Simple order-of-magnitude estimate

$$M_{A>140, Galaxy} = \left( \bar{M}_{NSNS} R_{NSNS} + \bar{M}_{NSBH} R_{NSBH} \right) \tau_{Galaxy}$$

- ▶ Constant rate throughout cosmic history
- ▶ Assumed distribution of binary masses and spins (for BHs) (from observations/ theory)
- ▶ ...
- ▶ Several estimates like this leading to similar conclusions – all making similar assumptions  
→ GCE models

Considering only heavy elements with  $A > 140$   
=> not clear how much of this material in GW170817



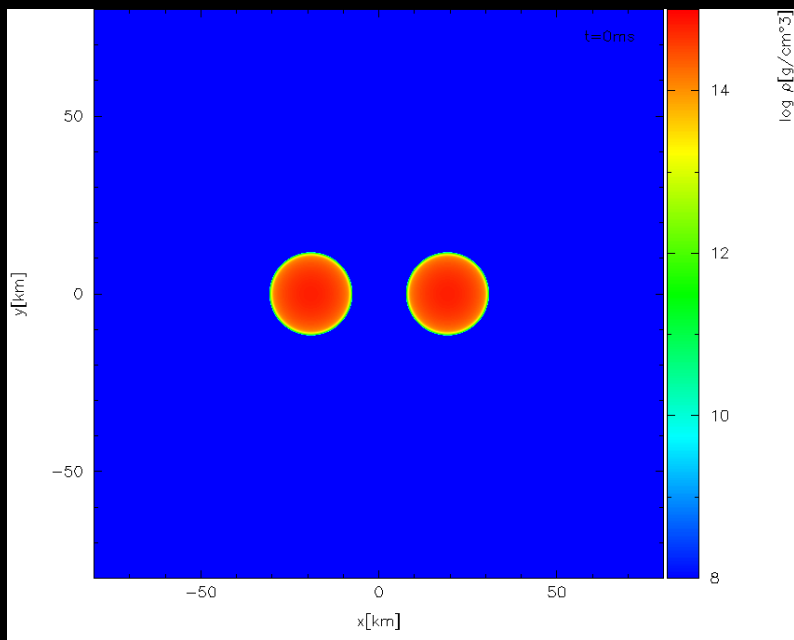
$M_{\text{ej}}(\text{NSNS})$ :  
Blue:  $10^{-3} M_{\text{sun}}$   
Red:  $3 \times 10^{-3} M_{\text{sun}}$   
Green:  $10^{-2} M_{\text{sun}}$

- ▶ Colored bands: rates for different EoSs
- ▶ Symbols: population synthesis predictions (Abadie et al. 2010)
- ▶ Vertical lines: pulsar observations (Kalogera et al. 2004)
- ▶ Dashed curve: short GRBs (Berger 2013)
- ▶ Arrow: volumetric rate (Abbott et al. 2017) converted to Galactic rate

- ▶ NS mergers are compatible with being dominant source of heavy elements  
(if only and early site has to be seen → Galactic chemical evolution)
- ▶ Certainly mergers play a prominent role in Galactic enrichment

NS radius constraints from collapse behavior

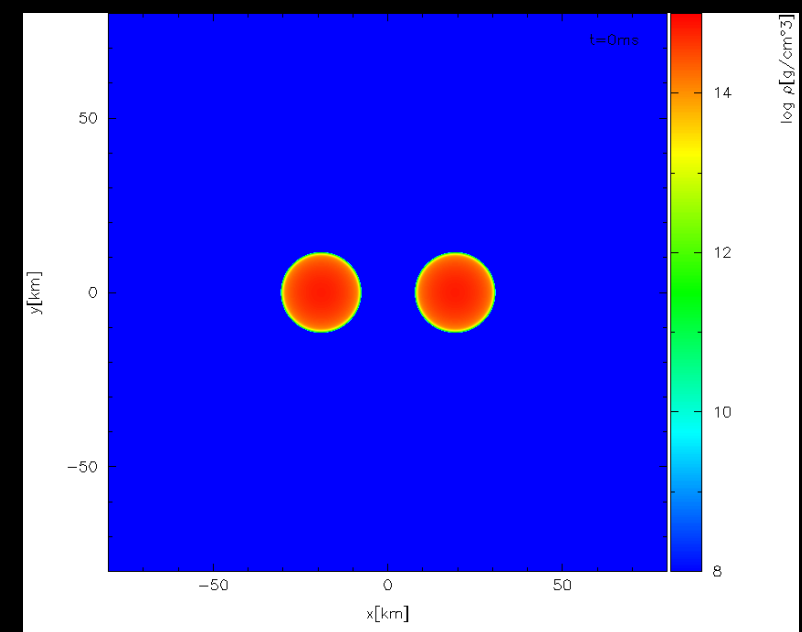




$$M_{\text{tot}} = 3.4 M_{\odot}$$



$$M_{\text{tot}} = 3.5 M_{\odot}$$



Shen EoS

## Collapse behavior: Prompt vs. delayed (/no) BH formation

Relevant for:

EoS constraints through  $M_{\text{max}}$  measurement

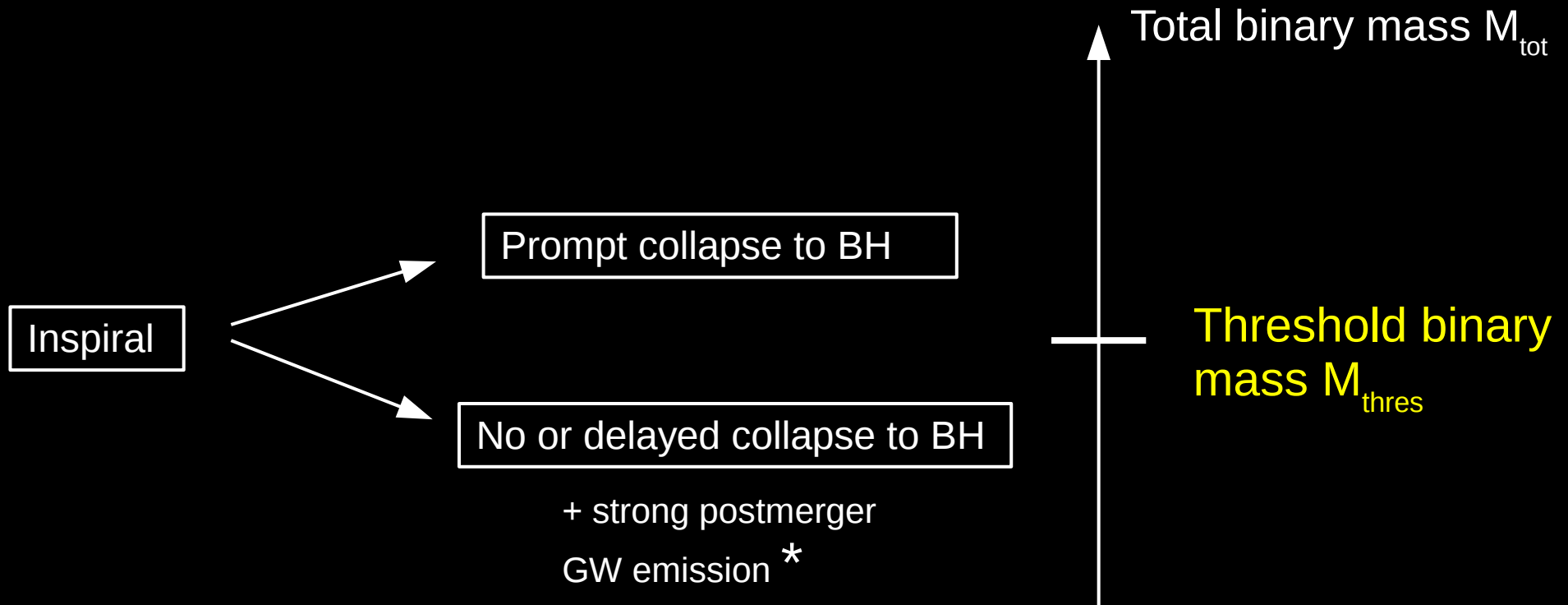
Conditions for short GRBs

Mass ejection

Electromagnetic counterparts powered by thermal emission

And NS radius constraints !!!

# Collapse behavior



\* not detected in GW170817 – not expected for given distance and current detector sensitivity

$M_{\text{thres}}$  EoS dependent - somehow  $M_{\text{max}}$  should play a role

# A simple but robust NS radius constraint from GW170817

- ▶ High ejecta mass inferred from electromagnetic transient
  - provides strong support for a delayed/no collapse in GW170817
  - even asymmetric mergers that directly collapse do not produce such massive ejecta

Reference	$m_{\text{dyn}} [M_{\odot}]$	$m_{\text{w}} [M_{\odot}]$
Abbott et al. (2017a)	0.001 – 0.01	–
Arcavi et al. (2017)	–	0.02 – 0.025
Cowperthwaite et al. (2017)	0.04	0.01
Chornock et al. (2017)	0.035	0.02
Evans et al. (2017)	0.002 – 0.03	0.03 – 0.1
Kasen et al. (2017)	0.04	0.025
Kasliwal et al. (2017b)	> 0.02	> 0.03
Nicholl et al. (2017)	0.03	–
Perego et al. (2017)	0.005 – 0.01	$10^{-5}$ – 0.024
Rosswog et al. (2017)	0.01	0.03
Smartt et al. (2017)	0.03 – 0.05	0.018
Tanaka et al. (2017a)	0.01	0.03
Tanvir et al. (2017)	0.002 – 0.01	0.015
Troja et al. (2017)	0.001 – 0.01	0.015 – 0.03

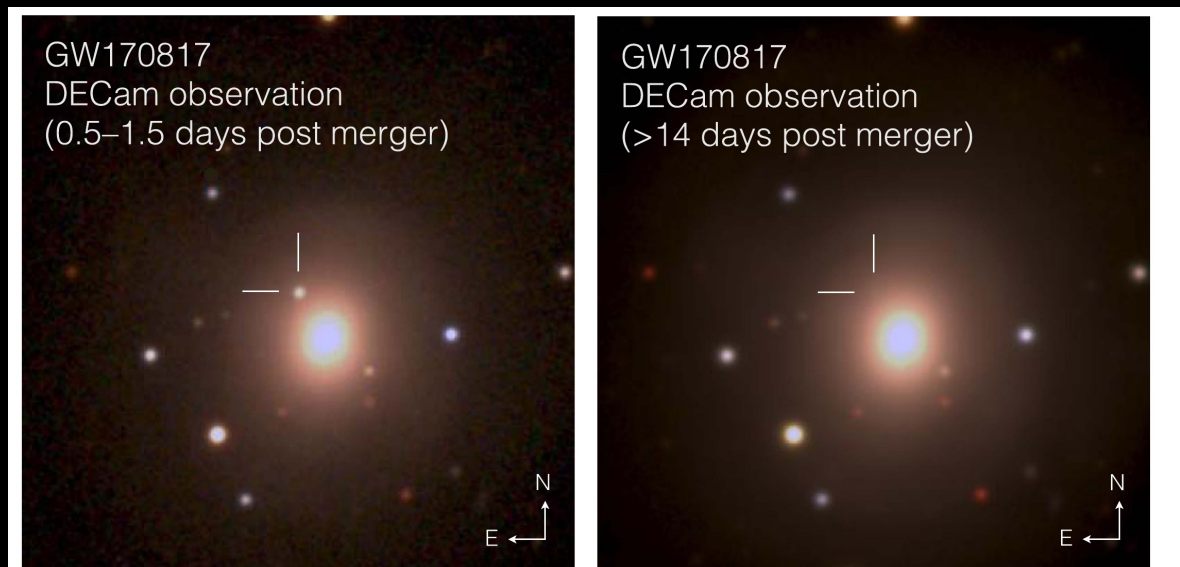
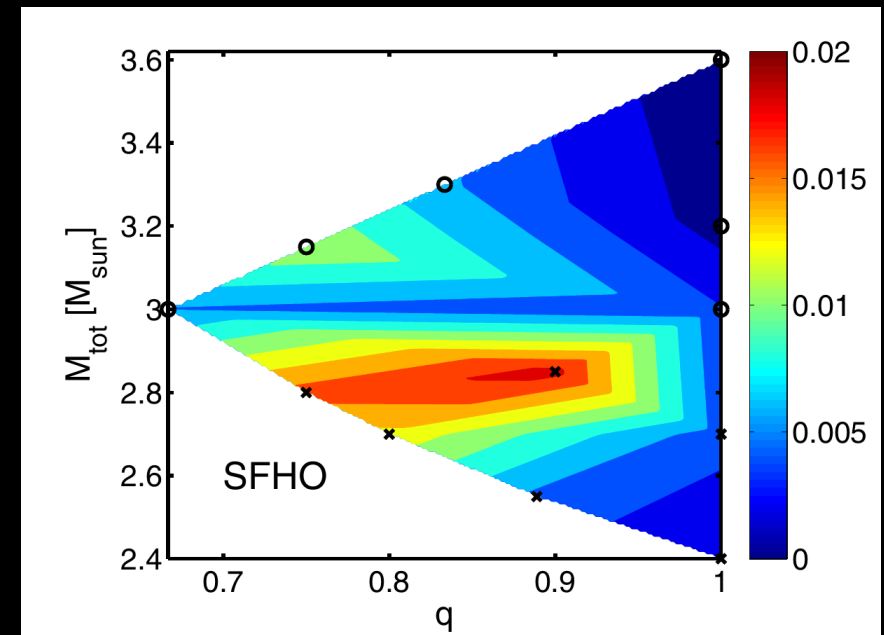
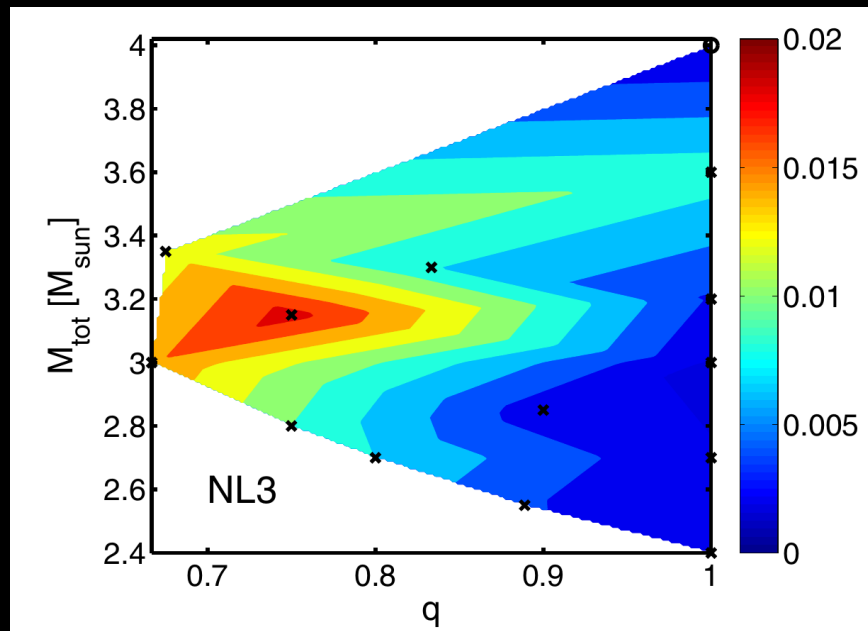
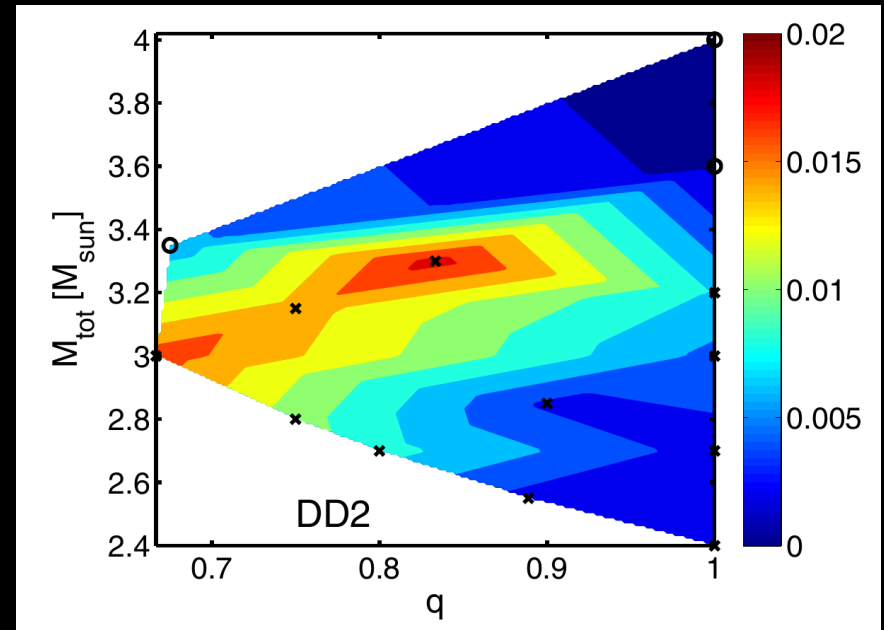


**Figure 1.** NGC4993  $g/r/z$  color composites ( $1'5 \times 1'5$ ). Left: composite of detection images, including the discovery  $z$  image taken on 2017 August 18 00:05:23 UT and the  $g$  and  $r$  images taken 1 day later; the optical counterpart of GW170817 is at R.A., decl. =197.450374,  $-23.381495$ . Right: the same area two weeks later.

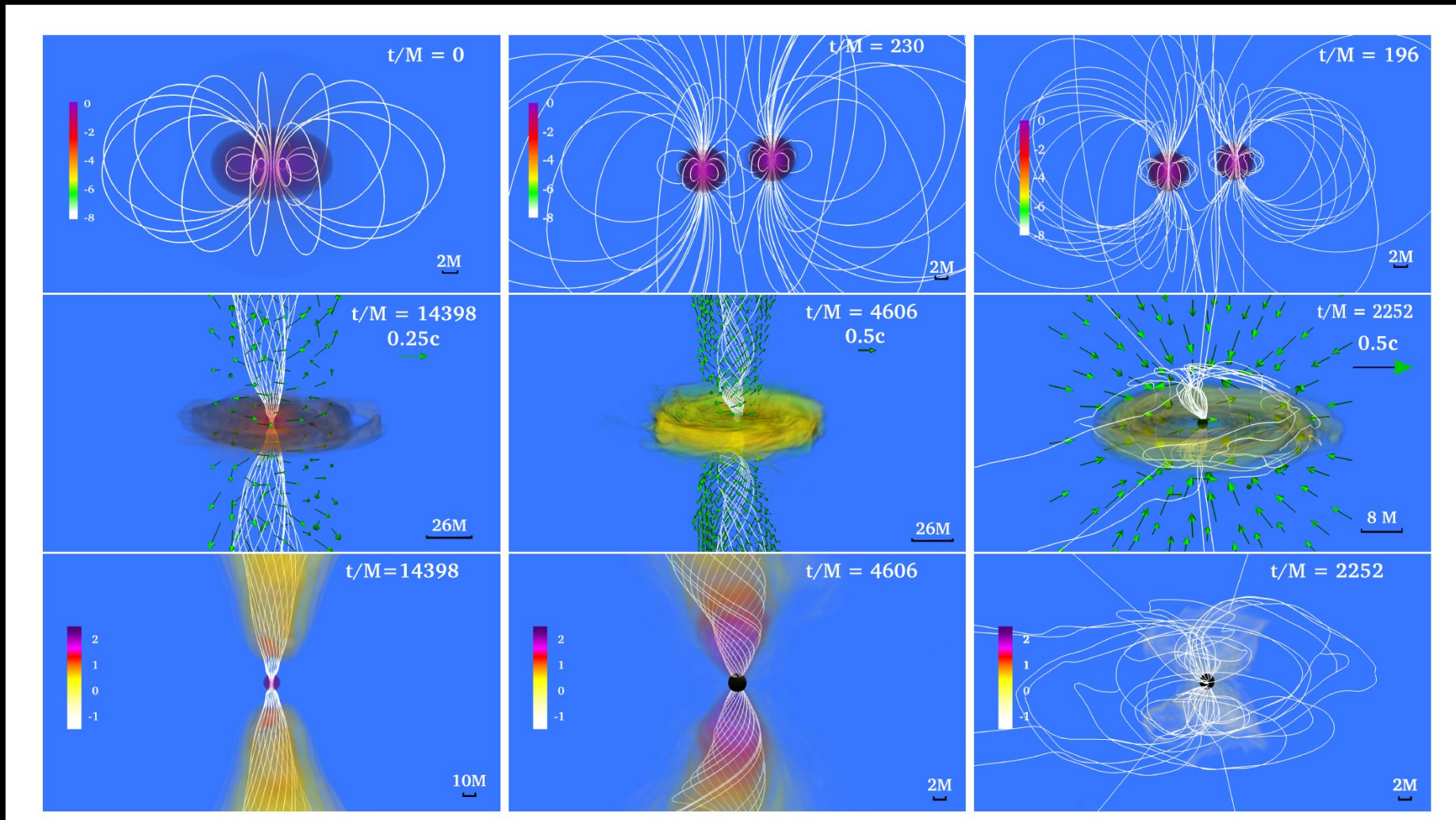
Soares-Santos et al 2017

- ▶ Ejecta masses depend on EoS and binary masses
- ▶ Note: high mass points already to soft EoS (tentatively/qualitatively)
- ▶ Prompt collapse leads to reduced ejecta mass
- ▶ Light curve depends on ejecta mass:  
→ 0.02 - 0.05  $M_{\text{sun}}$  point to delayed collapse
- ▶ Note: here only dynamical ejecta

Only dynamical ejecta

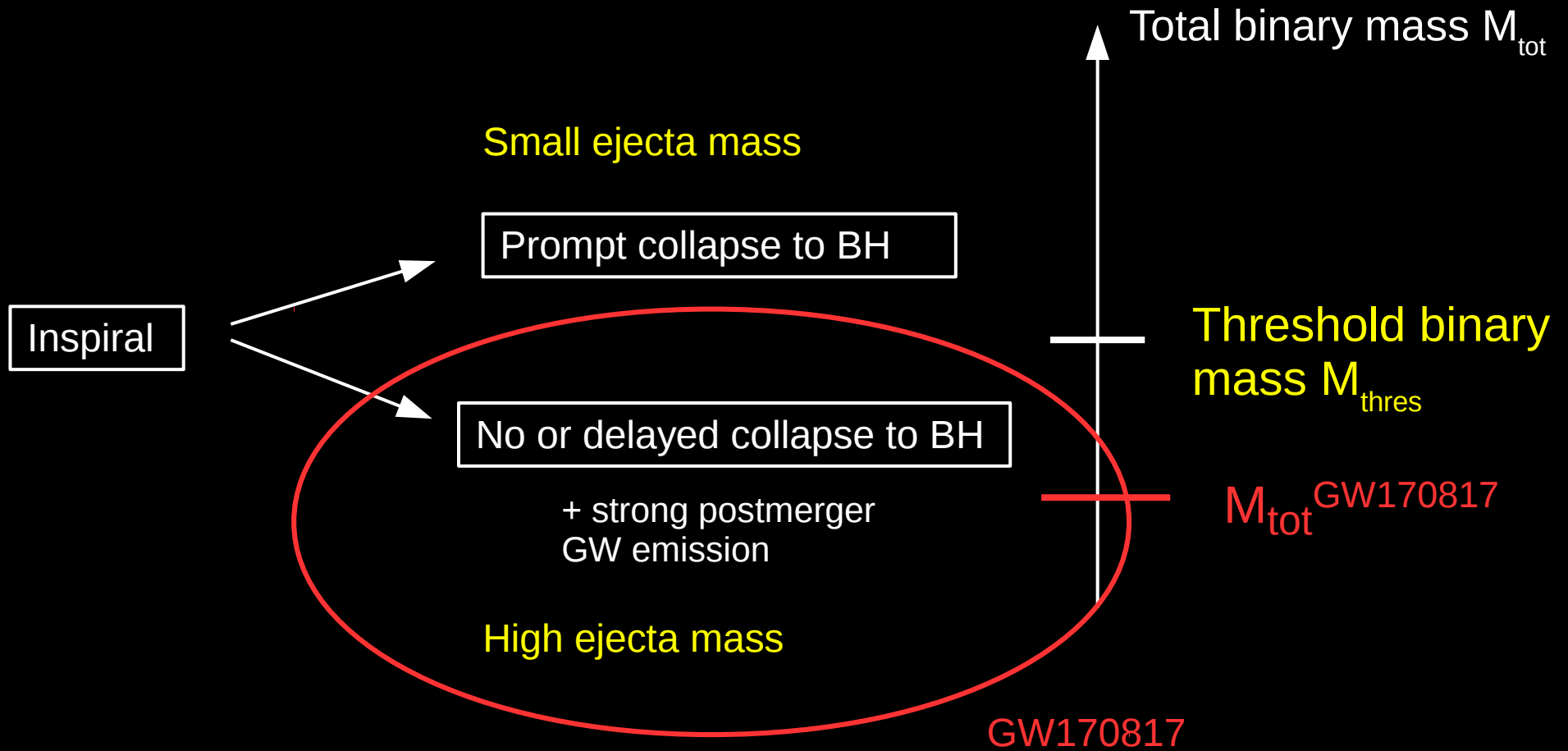


- ▶ GRB-like emission may be an argument for delayed collapse in GW170817



GRMHD simulations by Ruiz et al. 2017 suggest that delayed collapse required for jet formation

# Collapse behavior





# Simulations reveal $M_{\text{thres}}$

TOV properties of nonrotating stars, i.e. EoS characteristics

Merger property from simulations

EoS	$M_{\text{max}}$ ( $M_{\odot}$ )	$R_{\text{max}}$ (km)	$C_{\text{max}}$	$R_{1.6}$ (km)	$M_{\text{thres}}$ ( $M_{\odot}$ )
NL3 [37,38]	2.79	13.43	0.307	14.81	3.85
GS1 [39]	2.75	13.27	0.306	14.79	3.85
LS375 [40]	2.71	12.34	0.325	13.71	3.65
DD2 [38,41]	2.42	11.90	0.300	13.26	3.35
Shen [42]	2.22	13.12	0.250	14.46	3.45
TM1 [43,44]	2.21	12.57	0.260	14.36	3.45
SFHX [45]	2.13	10.76	0.292	11.98	3.05
GS2 [46]	2.09	11.78	0.262	13.31	3.25
SFHO [45]	2.06	10.32	0.294	11.76	2.95
LS220 [40]	2.04	10.62	0.284	12.43	3.05
TMA [44,47]	2.02	12.09	0.247	13.73	3.25
IUF [38,48]	1.95	11.31	0.255	12.57	3.05

Bauswein et al. 2013

Smooth particle hydrodynamics + conformal flatness

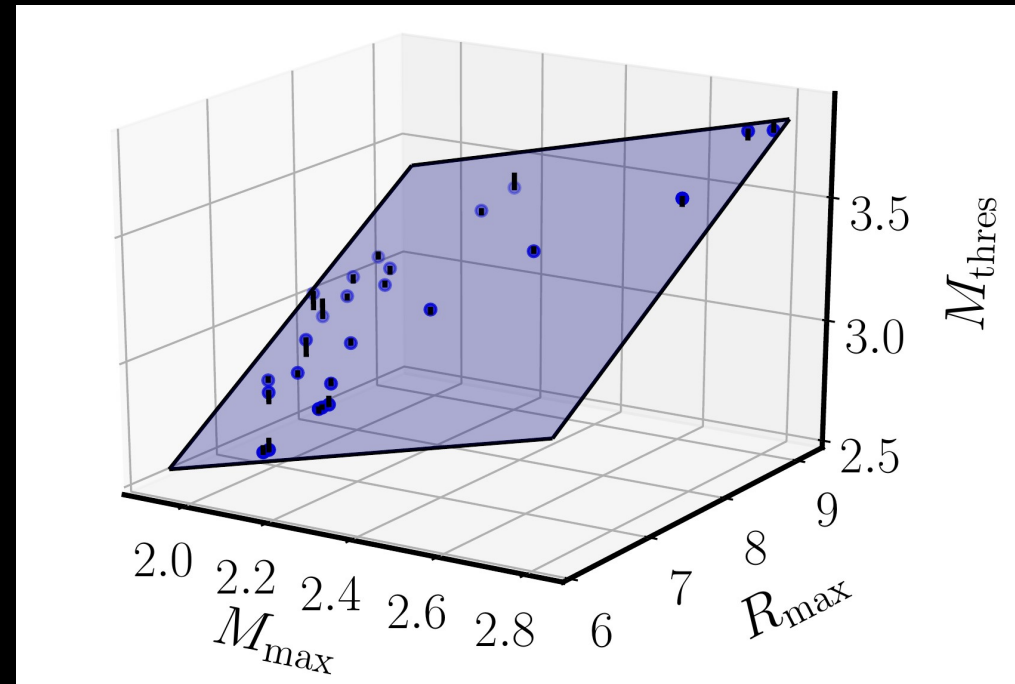
# Threshold binary mass

- ▶ Empirical relation from simulations with different  $M_{\text{tot}}$  and EoS
- ▶ Fits (to good accuracy):

$$M_{\text{thres}} = M_{\text{thres}}(M_{\text{max}}, R_{\text{max}}) = \left( -3.38 \frac{GM_{\text{max}}}{c^2 R_{\text{max}}} + 2.43 \right) M_{\text{max}}$$

$$M_{\text{thres}} = M_{\text{thres}}(M_{\text{max}}, R_{1.6}) = \left( -3.6 \frac{GM_{\text{max}}}{c^2 R_{1.6}} + 2.38 \right) M_{\text{max}}$$

- ▶ Both better than  $0.06 M_{\text{sun}}$



(1) If GW170817 was a delayed (/no) collapse:

$$M_{\text{thres}} > M_{\text{tot}}^{\text{GW170817}}$$

(2) Recall: empirical relation for threshold binary mass for prompt collapse:

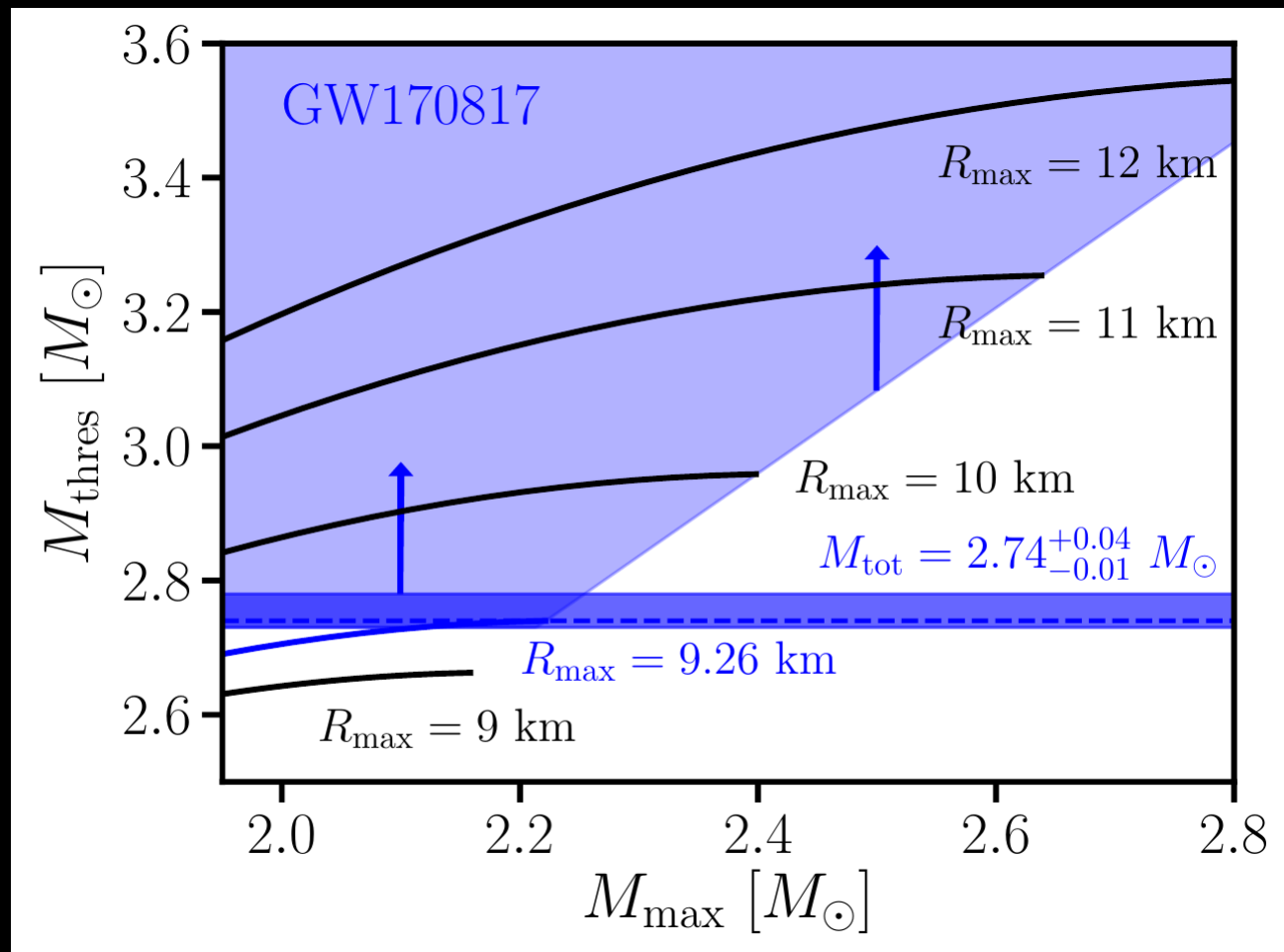
$$M_{\text{thres}} = \left( -3.38 \frac{G M_{\text{max}}}{c^2 R_{\text{max}}} + 2.43 \right) M_{\text{max}} > 2.74 M_{\odot} \quad (\text{with } M_{\text{max}}, R_{\text{max}} \text{ unknown})$$

(3) Causality: speed of sound  $v_s \leq c$   $\Rightarrow M_{\text{max}} \leq \frac{1}{2.82} \frac{c^2 R_{\text{max}}}{G}$

► Putting things together:

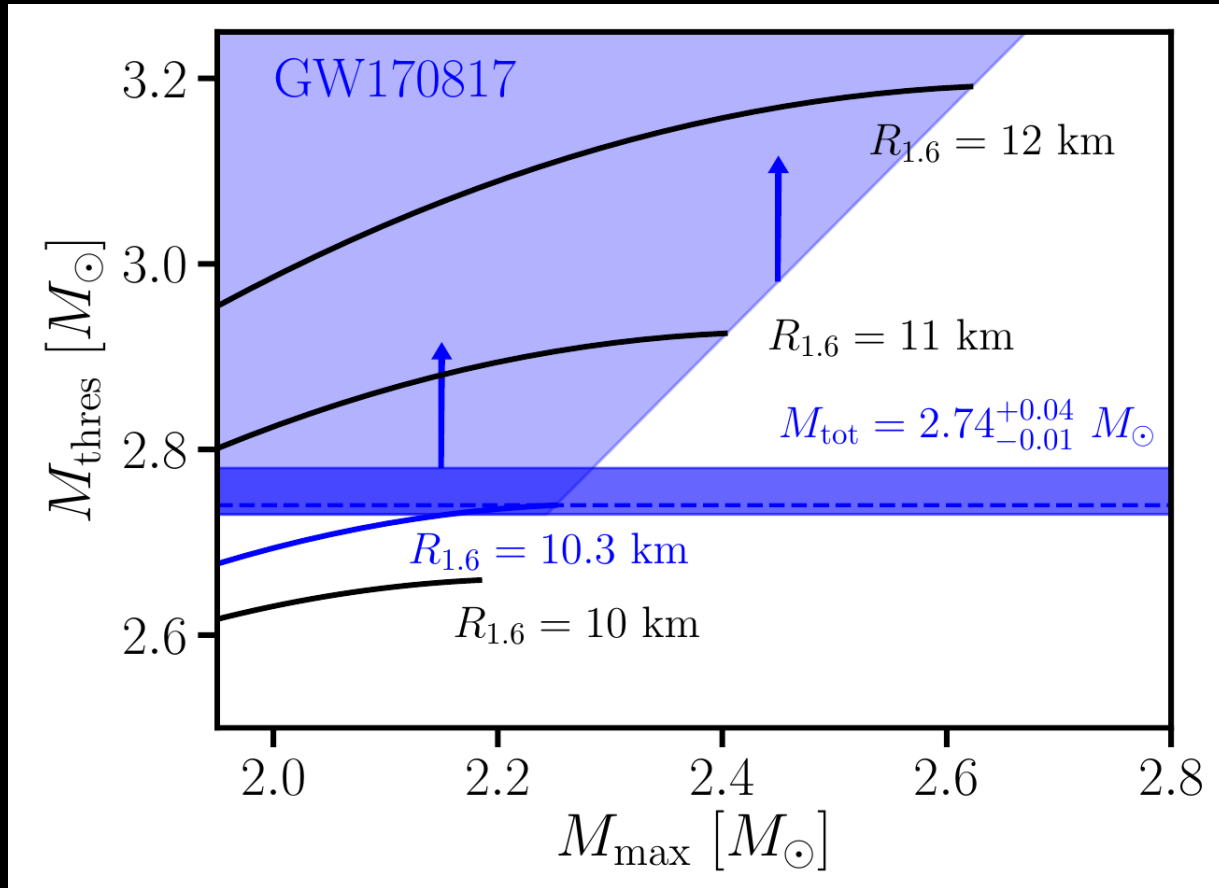
$$M_{\text{tot}}^{\text{GW170817}} \leq \left( -3.38 \frac{G M_{\text{max}}}{c^2 R_{\text{max}}} + 2.43 \right) M_{\text{max}} \leq \left( -\frac{3.38}{2.82} + 2.43 \right) \frac{1}{2.82} \frac{c^2 R_{\text{max}}}{G}$$

→ Lower limit on NS radius



$$M_{\text{thres}} = \left( -3.38 \frac{GM_{\text{max}}}{c^2 R_{\text{max}}} + 2.43 \right) M_{\text{max}}$$

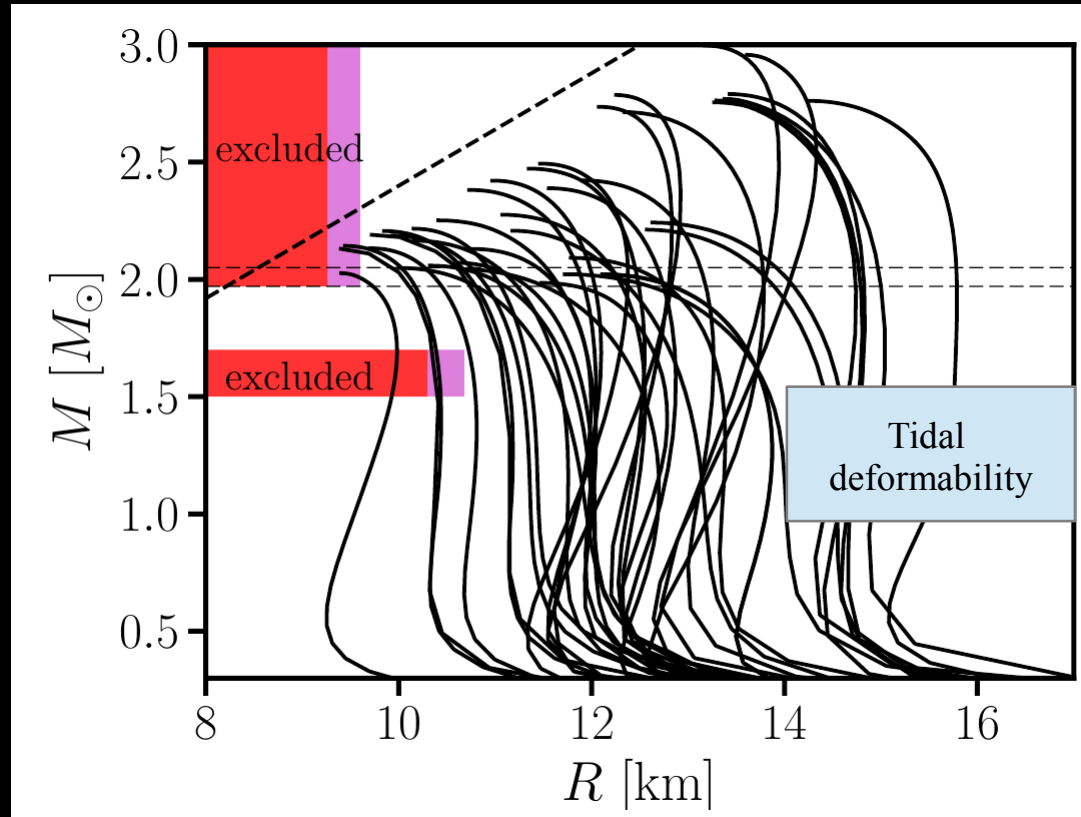
$$M_{\text{thres}} \geq 1.2 M_{\text{max}}$$



$$M_{\text{thres}} = \left( -3.6 \frac{G M_{\text{max}}}{c^2 R_{1.6}} + 2.38 \right) M_{\text{max}}$$

$$v_S = \sqrt{\frac{dP}{de}} \leq c \rightarrow M_{\text{max}} \leq \kappa R_{1.6} \Rightarrow M_{\text{thres}} \geq 1.2 M_{\text{max}}$$

# NS radius constraint from GW170817



Bauswein et al. 2017

- ▶  $R_{1.6} > 10.7$  km
- ▶ Excludes very soft nuclear matter



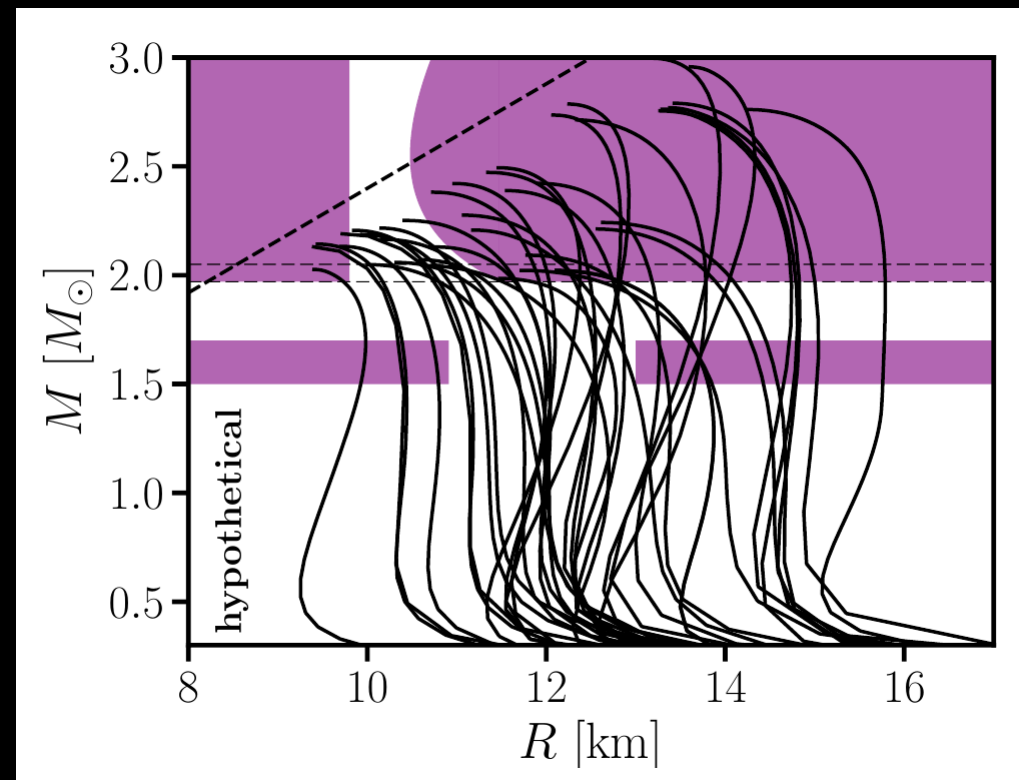
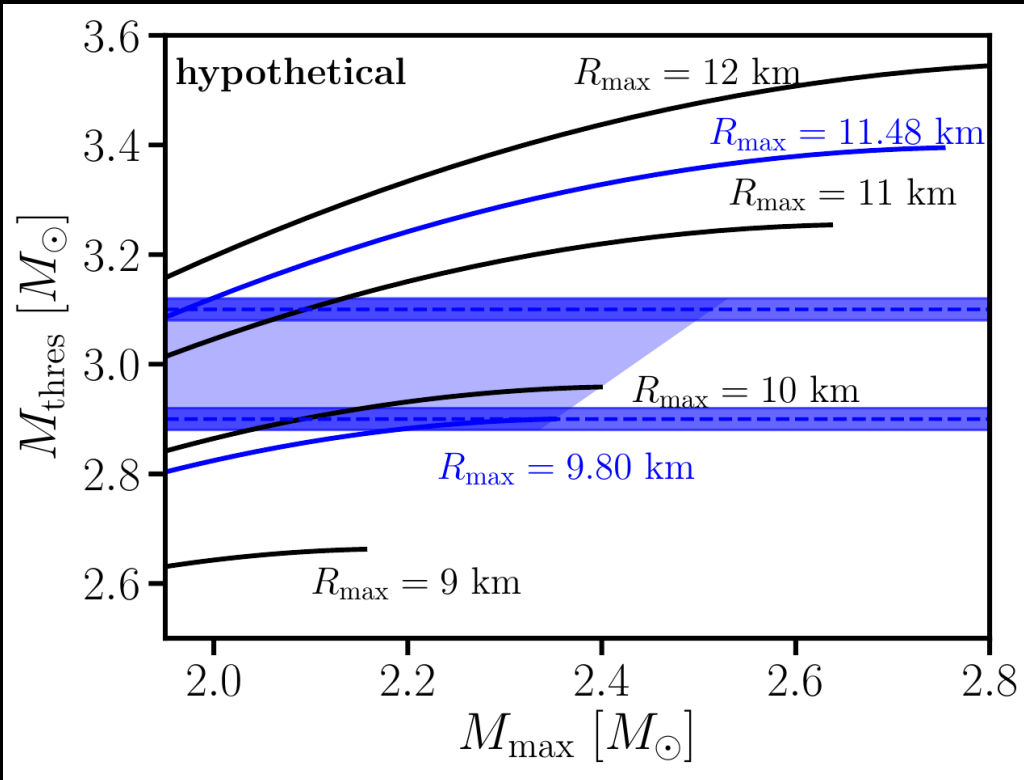
# Discussion - robustness

- ▶ Binary masses well measured with high confidence error bar
- ▶ Clearly defined working hypothesis: delayed collapse
  - testable by refined emission models
  - as more events are observed more robust distinction
- ▶ Very conservative estimate, errors can be quantified
- ▶ Empirical relation can be tested by more elaborated simulations (but unlikely that MHD or neutrinos can have strong impact on  $M_{\text{thres}}$ )
- ▶ Confirmed by semi-analytic collapse model
- ▶ Low-SNR constraint !!!

# Future

- ▶ Any new detection can be employed if it allows distinction between prompt/delayed collapse
- ▶ With more events in the future our comprehension of em counterparts will grow → more robust discrimination of prompt/delayed collapse events
- ▶ Low-SNR detections sufficient !!! → that's the potential for the future
  - we don't need louder events, but more
  - complimentary to existing ideas for EoS constraints

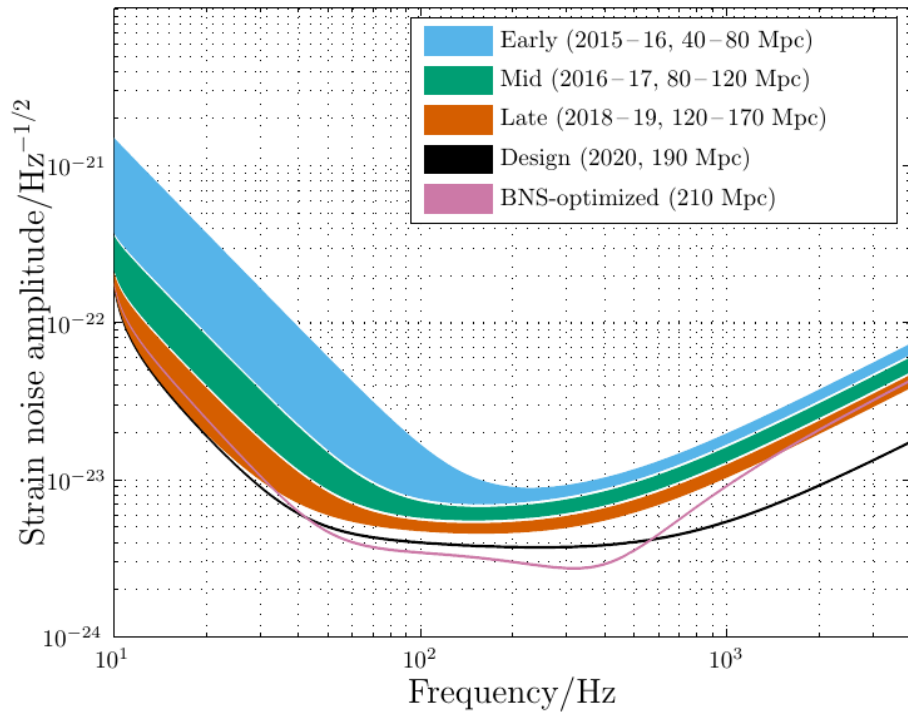
# Future detections (hypothetical discussion)



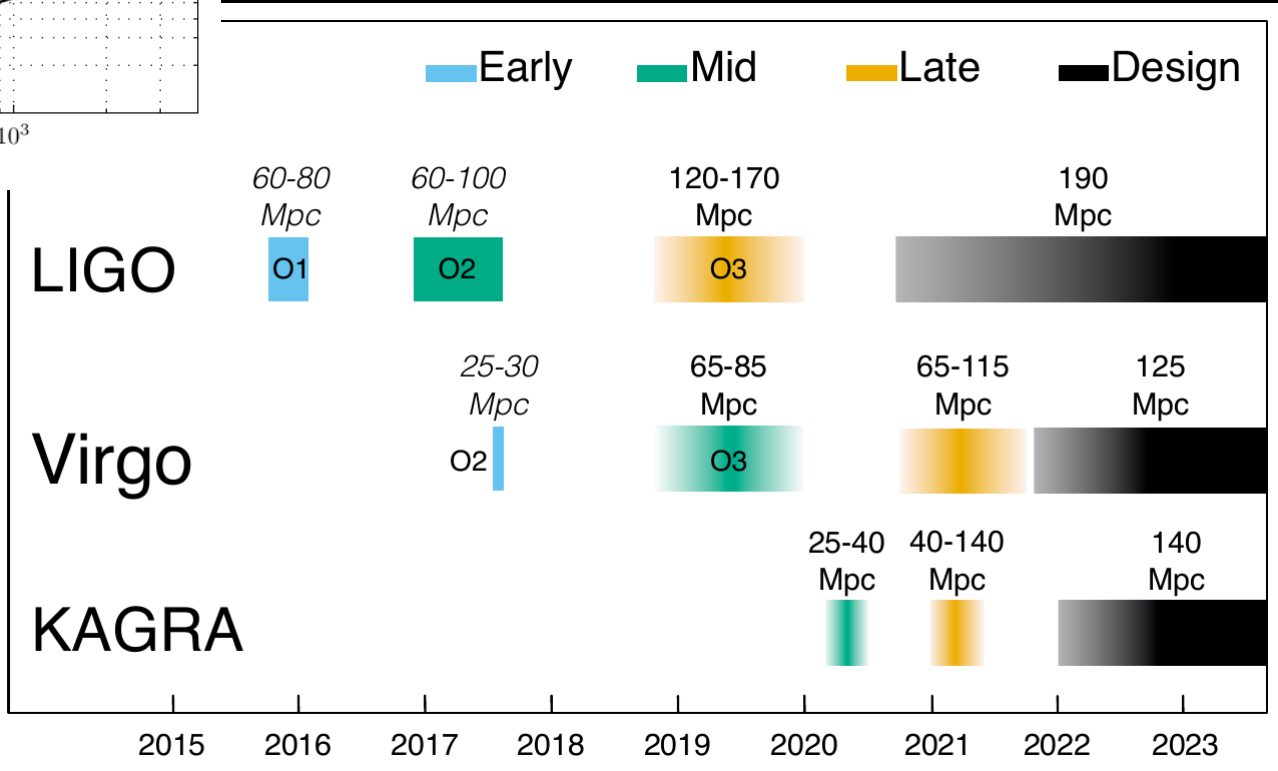
- as more events are observed, bands converge to true  $M_{\text{thres}}$
- prompt collapse constrains  $M_{\text{max}}$  from above

# Future plans

Advanced LIGO



Abbott et al. 2017



# Future: Maximum mass

- ▶ Empirical relation

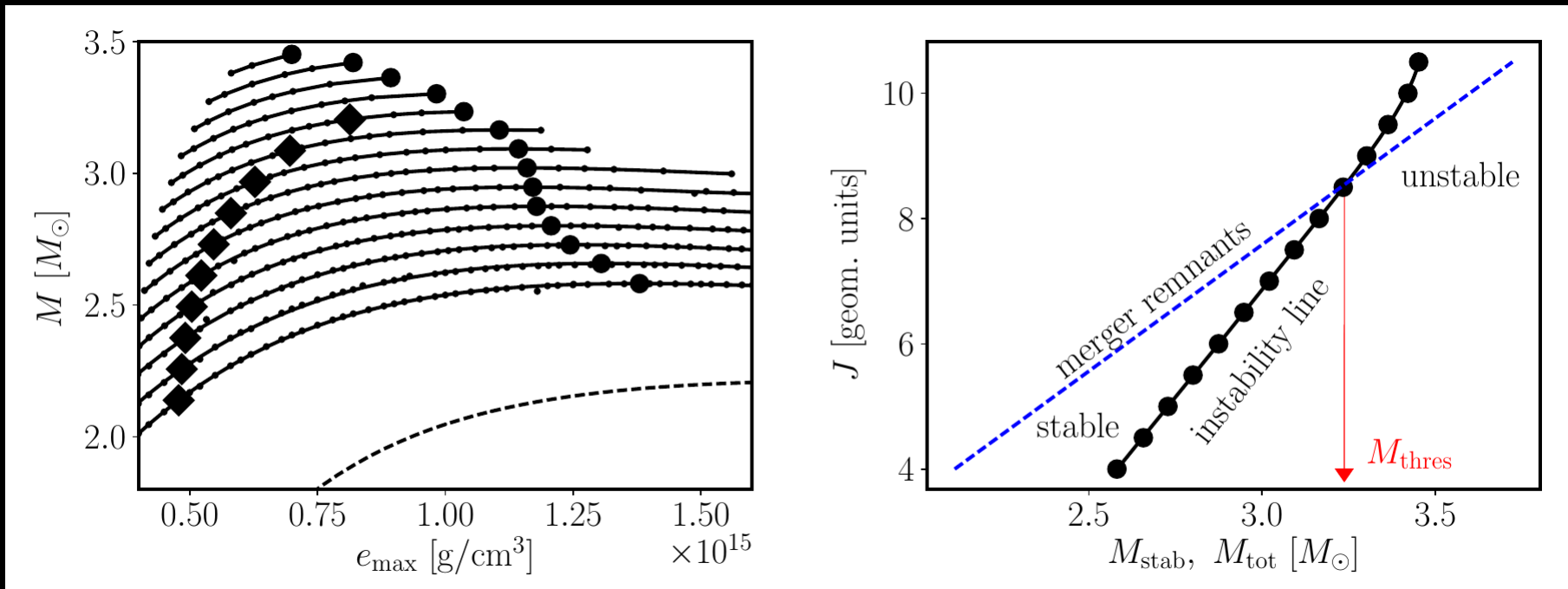
$$M_{\text{thres}} = \left( -3.6 \frac{G M_{\text{max}}}{c^2 R_{1.6}} + 2.38 \right) M_{\text{max}}$$

- ▶ Sooner or later we'll know  $R_{1.6}$  (e.g. from postmerger) and  $M_{\text{thres}}$  (from several events – through presence/absence of postmerger GW emission or em counterpart)

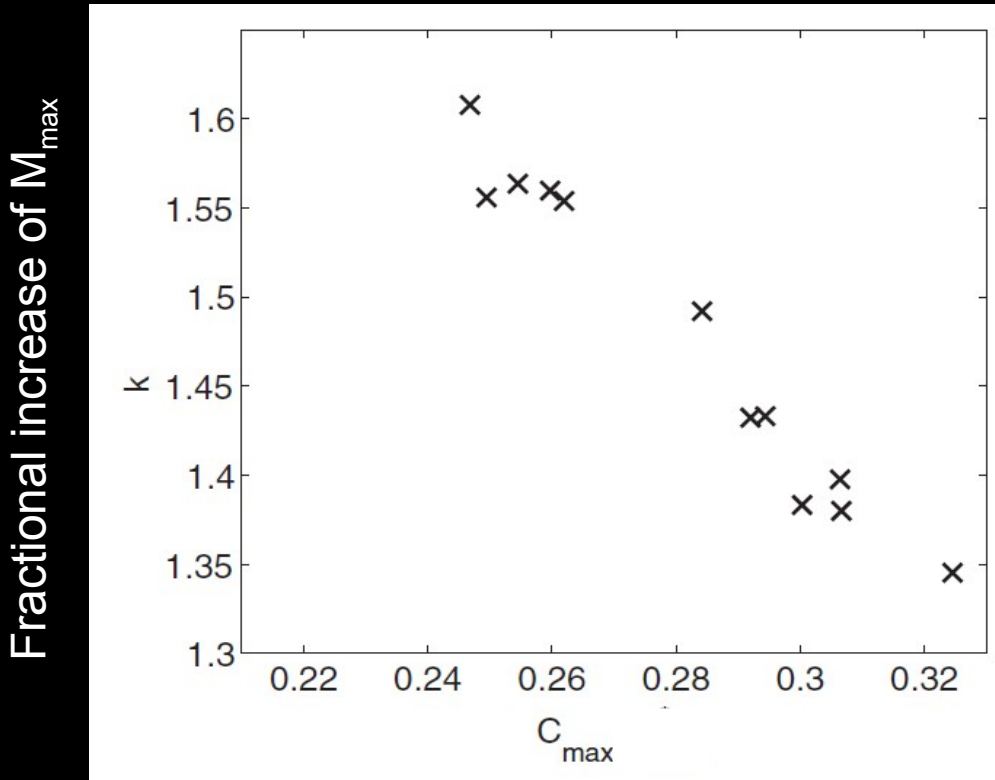
=> direct inversion to get precise estimate of  $M_{\text{max}}$

# Semi-analytic model: details

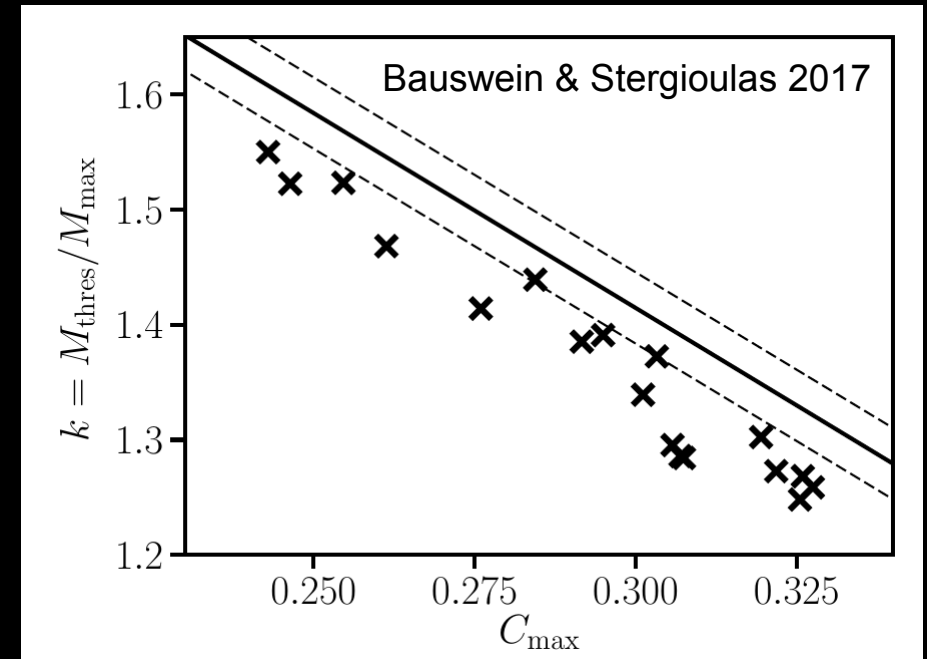
- ▶ Stellar equilibrium models computed with RNS code (diff. Rotation,  $T=0$ , many different microphysical EoS) => turning points =>  $M_{\text{stab}}(J)$
- ▶ Compared to  $J(M_{\text{tot}})$  of merger remnants from simulations (very robust result) → practically independent from simulations



# Semi-analytic model reproducing collapse behavior



Bauswein et al 2013: numerical determination of collapse threshold through hydrodynamical simulations



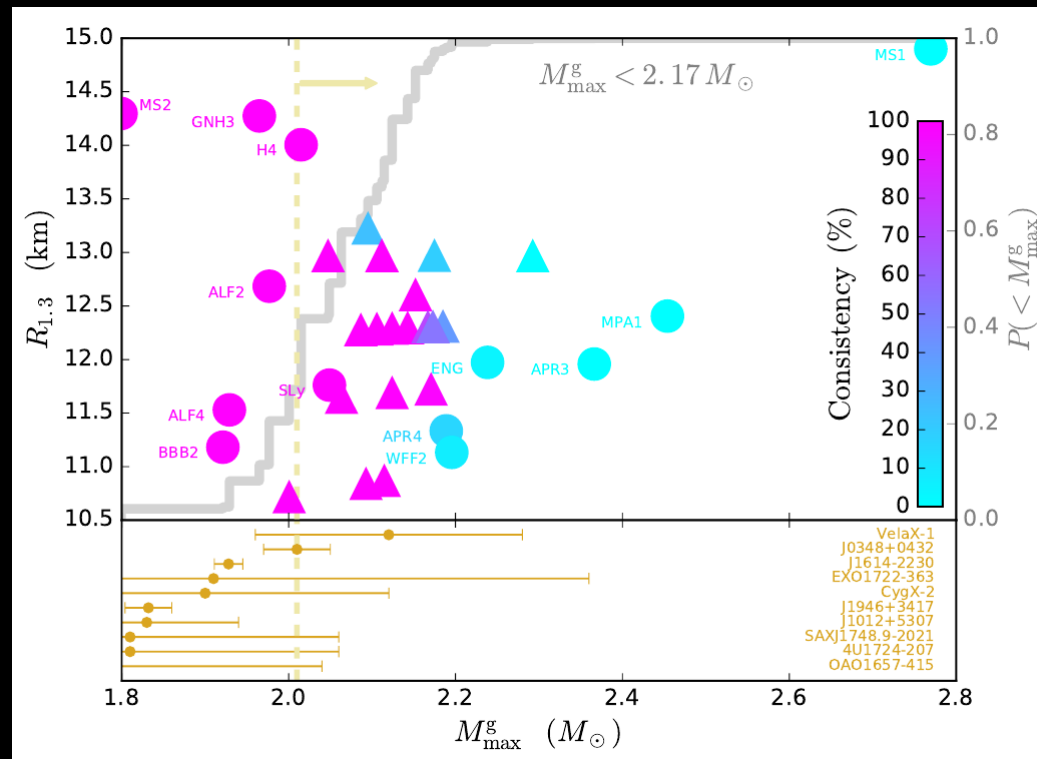
Solid line fit to numerical data

Crosses stellar **equilibrium models**:

- prescribed (simplistic) diff. rotation
- many EoSs at  $T=0$
- detailed angular momentum budget !  
=> equilibrium models qualitatively reproduce collapse behavior
- even quantitatively good considering the adopted approximations

# $M_{\max}$ from GW170817

- ▶ Arguments: no prompt collapse; no long-lasting pulsar spin-down (too less energy deposition)
- ▶ If GW170817 did not form a supramassive NS (rigidly rotating  $> M_{\max}$ )  
→  $M_{\max} < \sim 2.2-2.4 M_{\text{sun}}$  (relying on some assumption)





# Summary

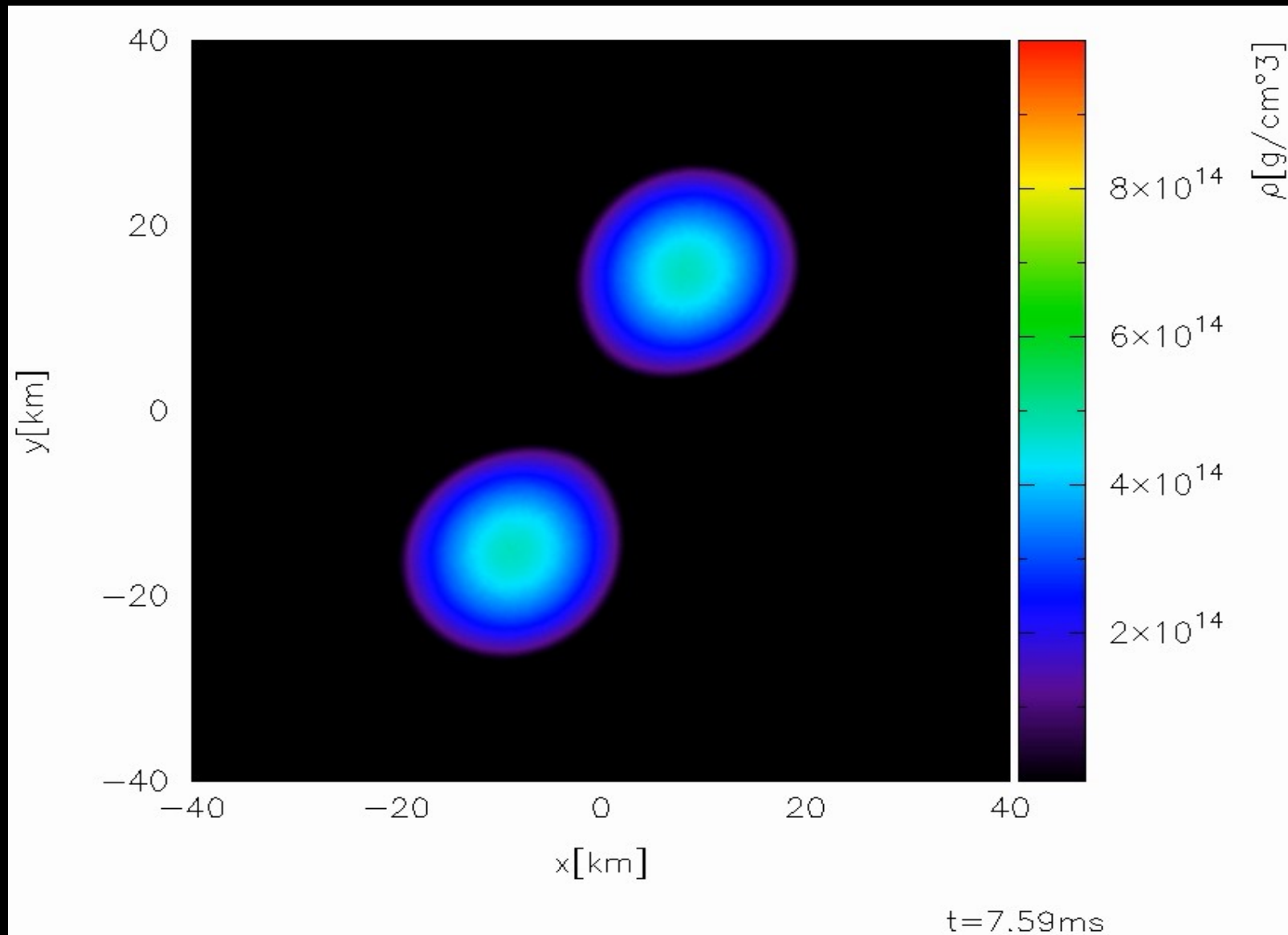
- ▶ Strong evidence for rapid neutron capture process in ejecta of NS mergers
- ▶ Light curve properties of GW170817 in ballpark of theoretical models
- ▶ Estimated rates are compatible with mergers being the dominant contributor of heavy elements
- ▶ High ejecta mass in GW170817 suggest no direct collapse of the remnant
- ▶ Measured total binary mass constrains threshold mass for prompt collapse
- ▶ Robust lower limit on NS radii:  $R > 10.7 \text{ km}$  for  $1.6 M_{\text{sun}}$
- ▶ Rules out very soft nuclear matter
- ▶ A lot of potential for future when similar events become available  
(in particular from prompt collapse  $\rightarrow$  upper limit on  $R$  and  $M_{\text{max}}$ )

# Postmerger GW emission\*

(dominant frequency of postmerger phase)

\* not detected for GW170817 – but expected for current sensitivity and  $d=40$  Mpc  
(Abbott et al. 2017)

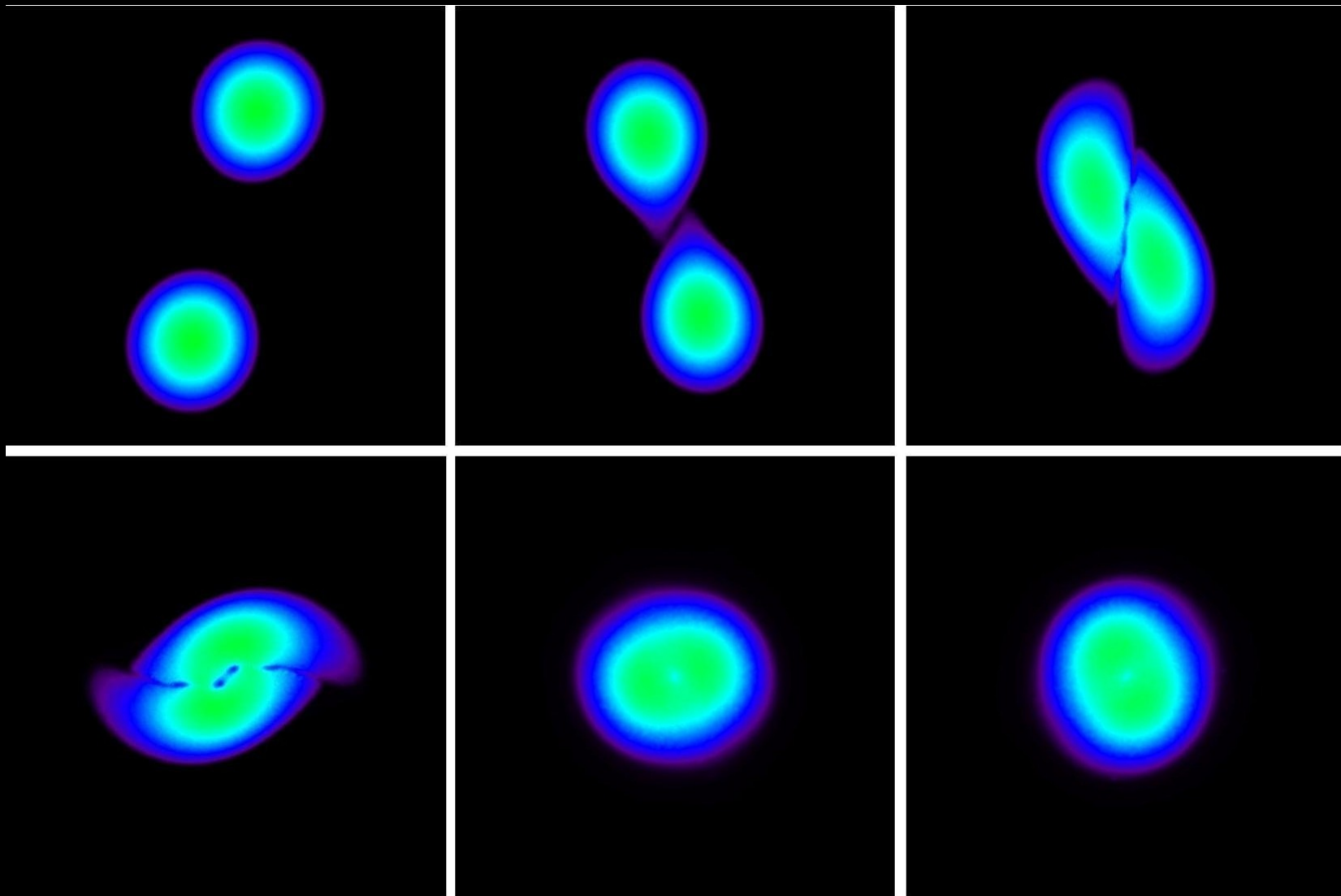
# Simulation: $1.35+1.35 M_{\text{sun}}$



Density evolution in equatorial plane, Shen EoS

Relativistic smooth particle hydrodynamics, conformally flat spatial metric, microphysical temperature-dependent EoS

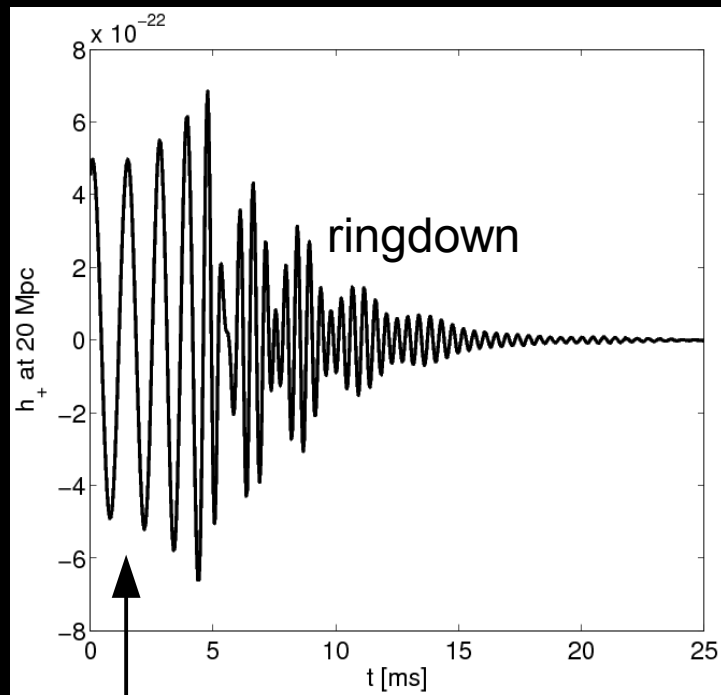
1.35-1.35 Msun, Shen EoS



Relativistic smooth particle hydrodynamics, conformally flat spatial metric,  
microphysical temperature-dependent EoS

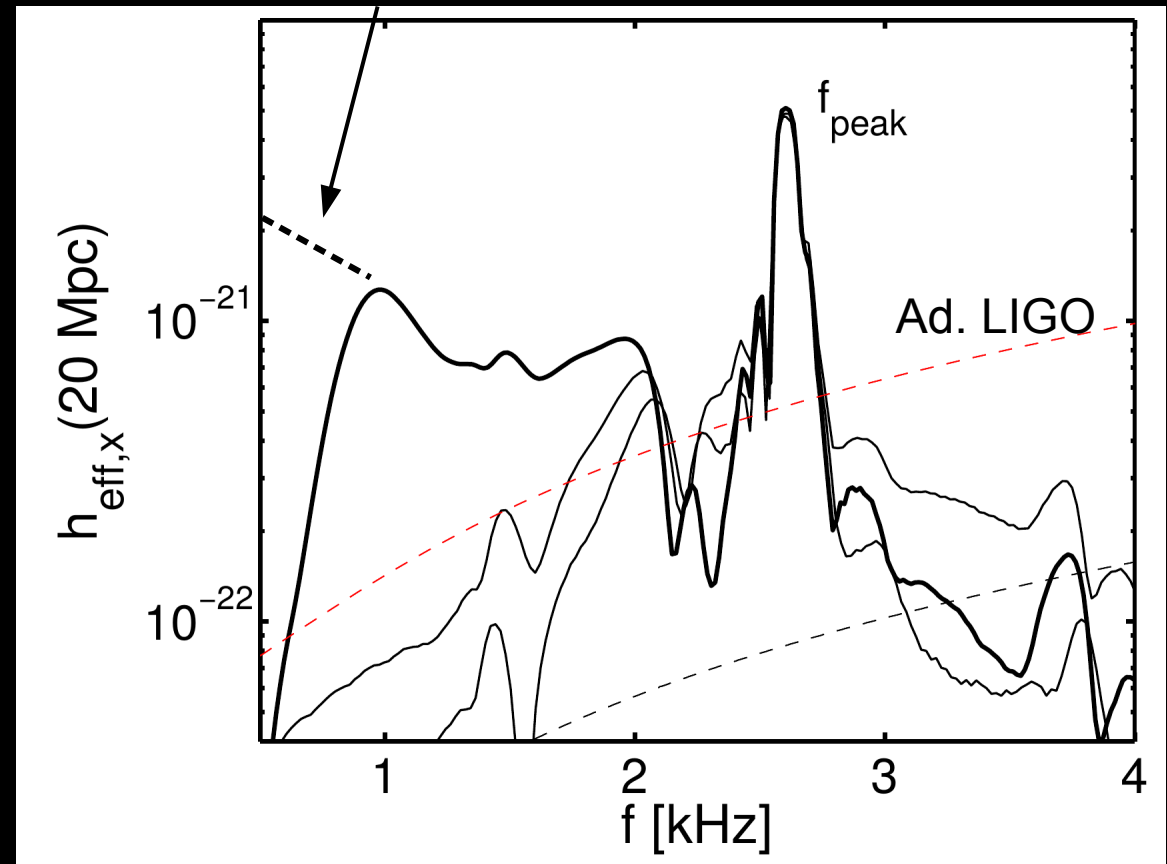
# Postmerger

1.35-1.35  $M_{\text{sun}}$ , 20 Mpc



Earlier inspiral

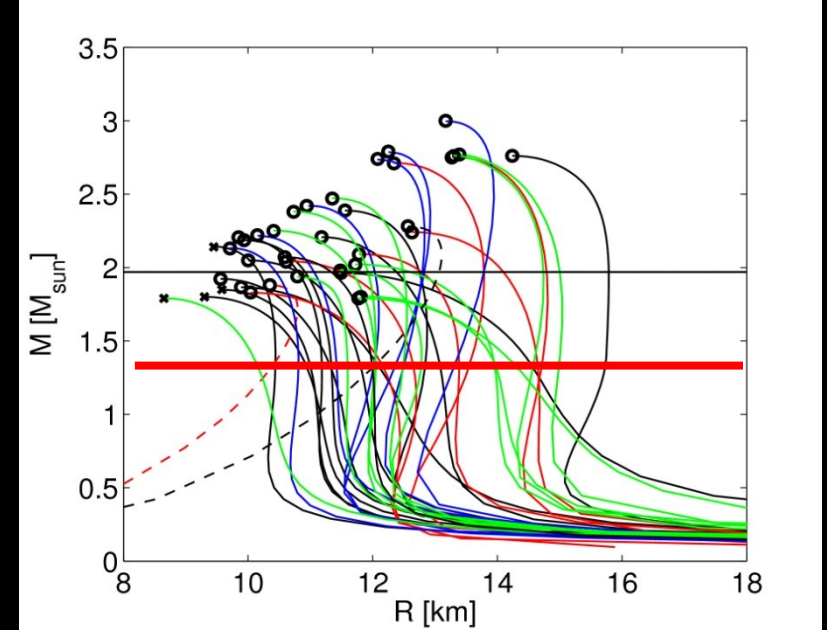
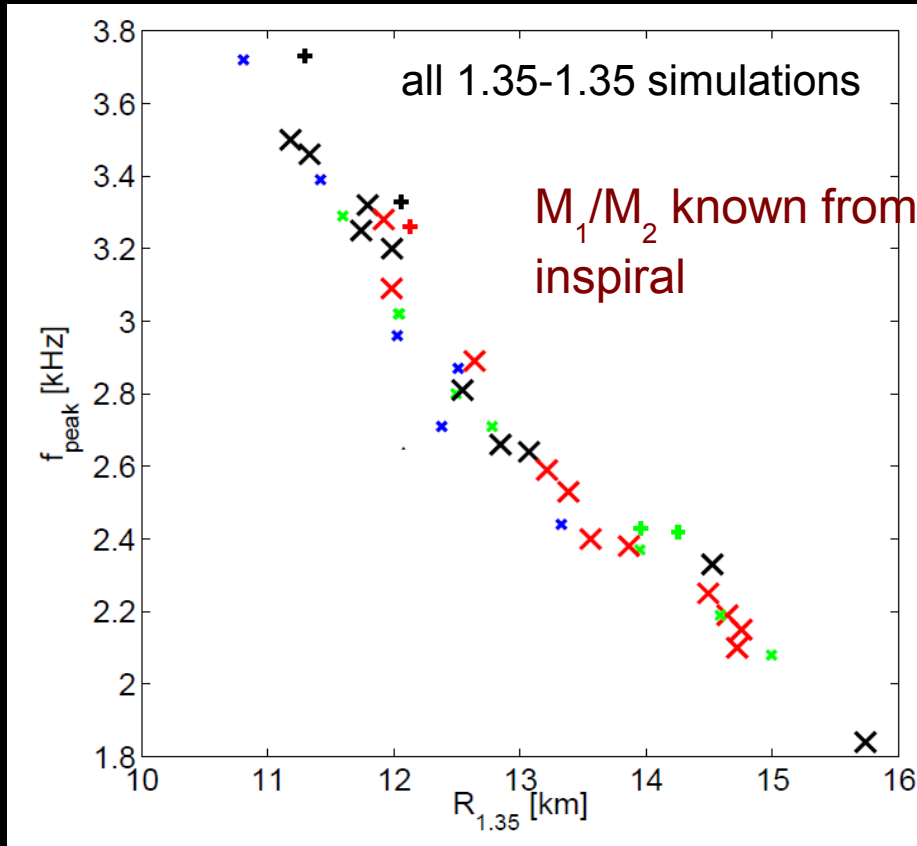
EoS



Dominant postmerger oscillation frequency  $f_{\text{peak}}$

Very characteristic (robust feature in all models)

Every data point a single simulation of a  $1.35\text{-}1.35 M_{\text{sun}}$  binary



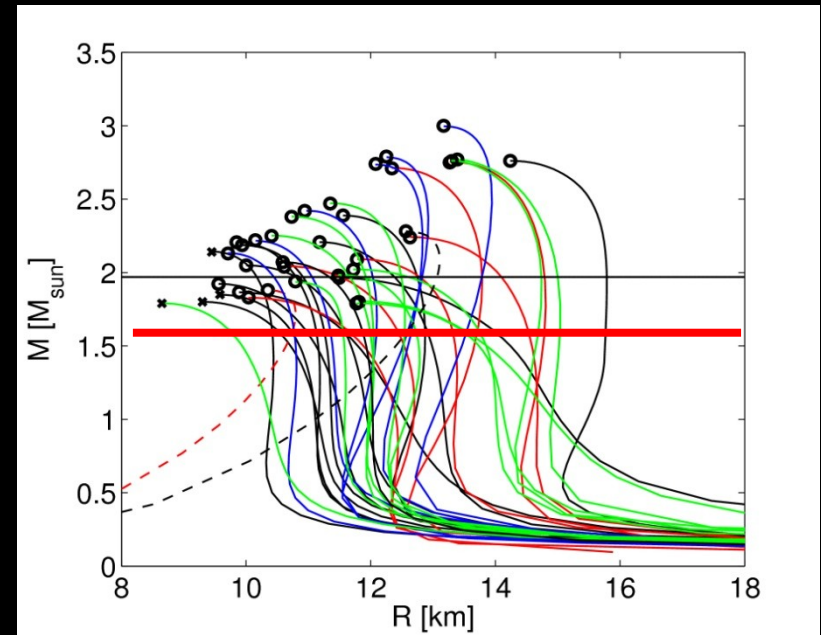
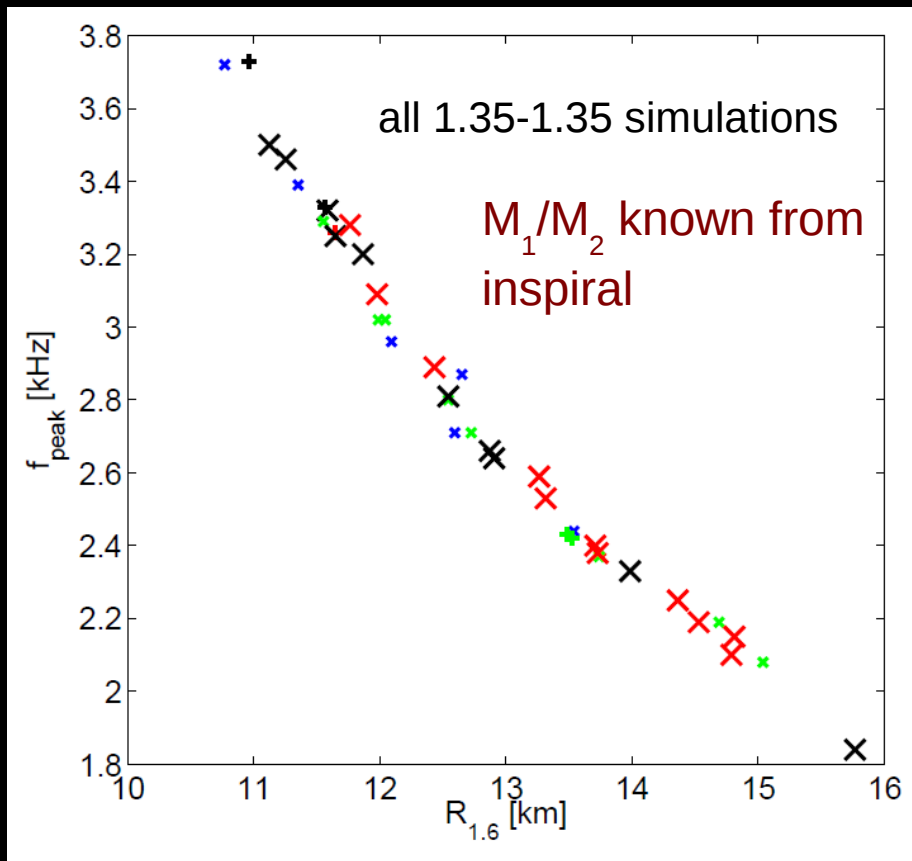
characterize EoS by radius of nonrotating NS with  $1.35 M_{\text{sun}}$

Bauswein et al. 2012

Pure TOV property => **Radius measurement** via  $f_{\text{peak}}$

→ **Empirical relation between GW frequency and NS radius (= our EoS parameter)**

Important: Simulations for the same binary mass, but with varied EoS  
Recall that total mass can be measured quite accurately



characterize EoS by radius of nonrotating NS with  $1.6 M_{\text{sun}}$

Bauswein et al. 2012

Pure TOV/EoS property => **Radius measurement** via  $f_{\text{peak}}$

Fit:  $R(1.6 M_{\odot}) = 1.1 f_{GW}^2 - 8.6 f_{GW} + 28.$

Important: Simulations for the same binary mass, just with varied EoS

# Causal limit

